Supplementary Information

Azadipyrromethene Dye Derivatives in Coordination Chemistry: Structure-Properties Relationship of Homoleptic M(II) Complexes

*André Bessette [1,2], Janaina G. Ferreira [1], Martin Giguère [2], Francis Bélanger [2], Denis Désilets [2] and Garry S. Hanan [1] *.*

[1] Département de Chimie, Université de Montréal, Pavillon J.-A. Bombardier, 5155 Decelles Avenue, Montréal, Québec, H3T-2B1, Canada

[2] Saint-Jean Photochimie Inc., 725 Trotter Street, Saint-Jean-sur-Richelieu, Québec, J3B 8J8, Canada.

Figure S.1 – HR-ESIMS of compound **2b** and its fitting with theoretical spectrum.

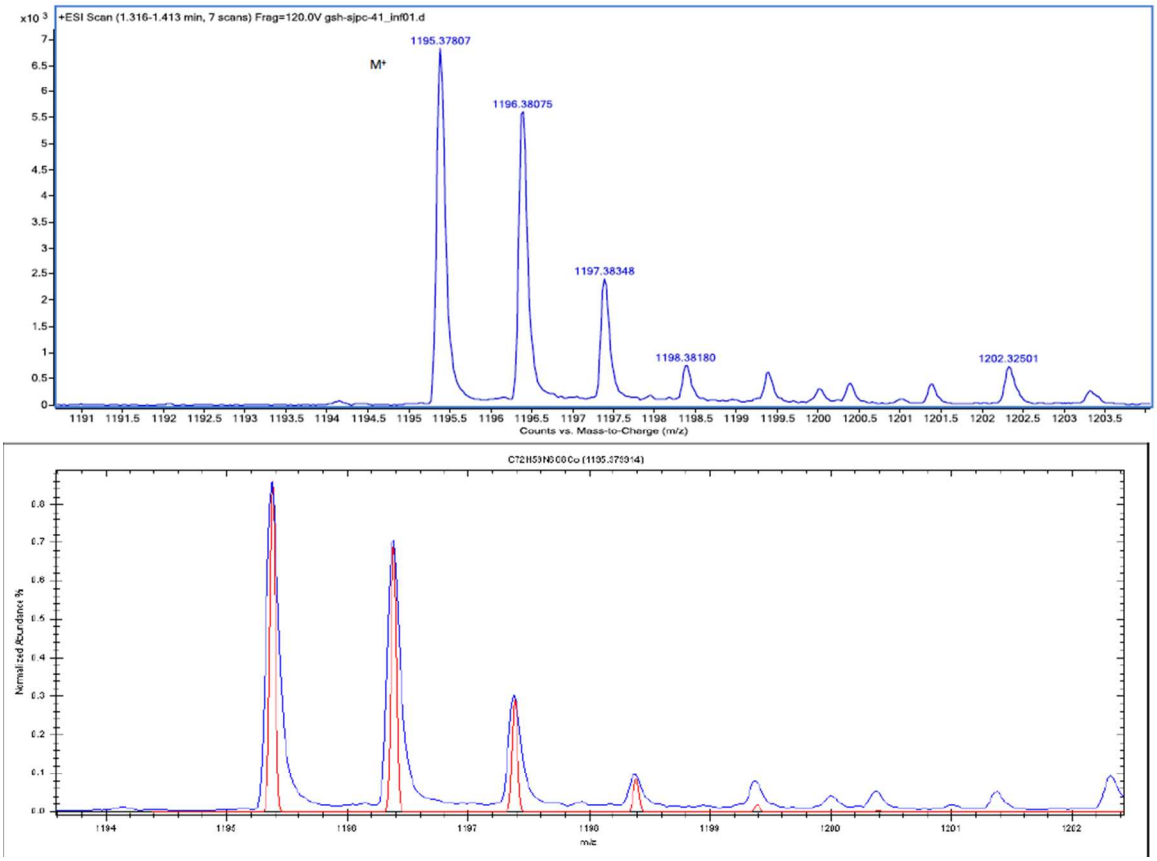

Figure S.2 – HR-ESIMS of compound **3b** and its fitting with theoretical spectrum.

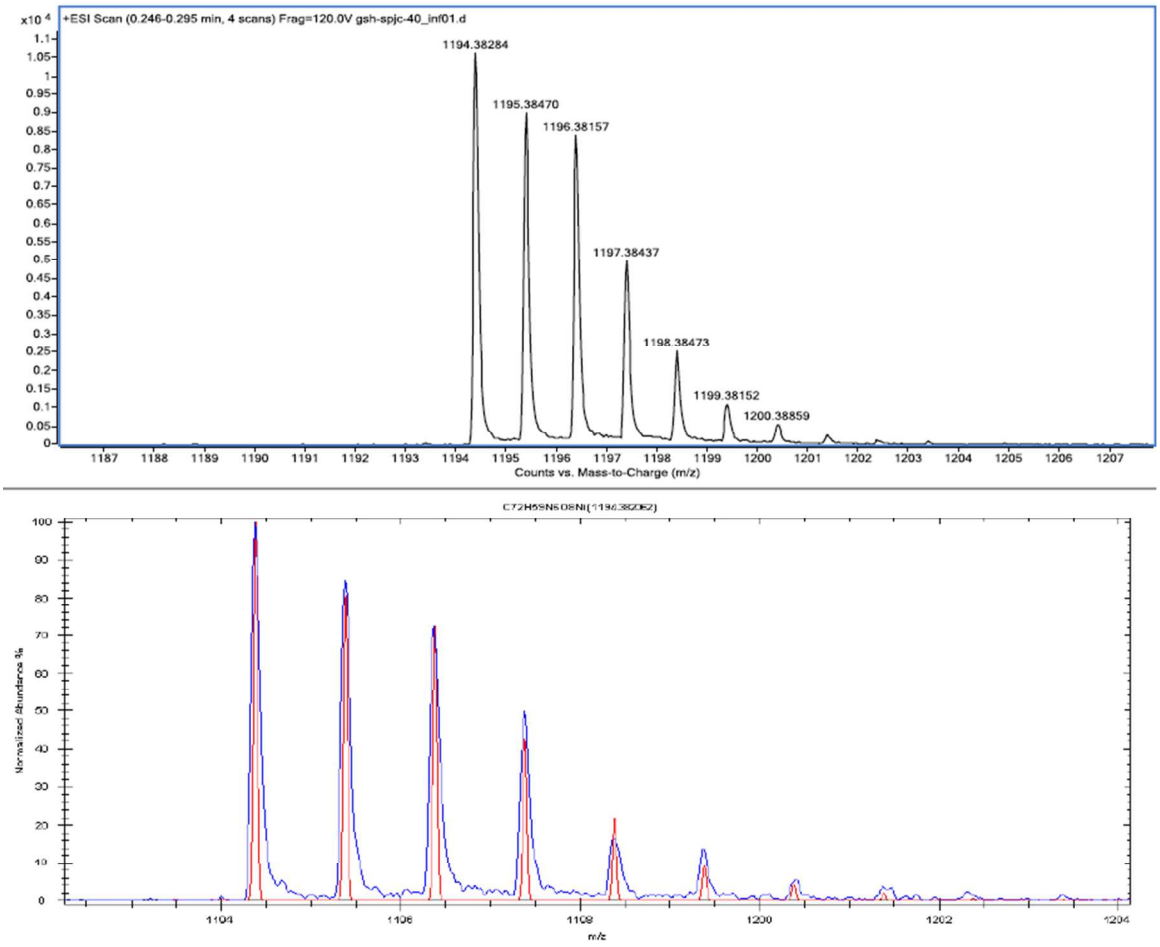

Figure S.3 – HR-ESIMS of compound **4b** and its fitting with theoretical spectrum.

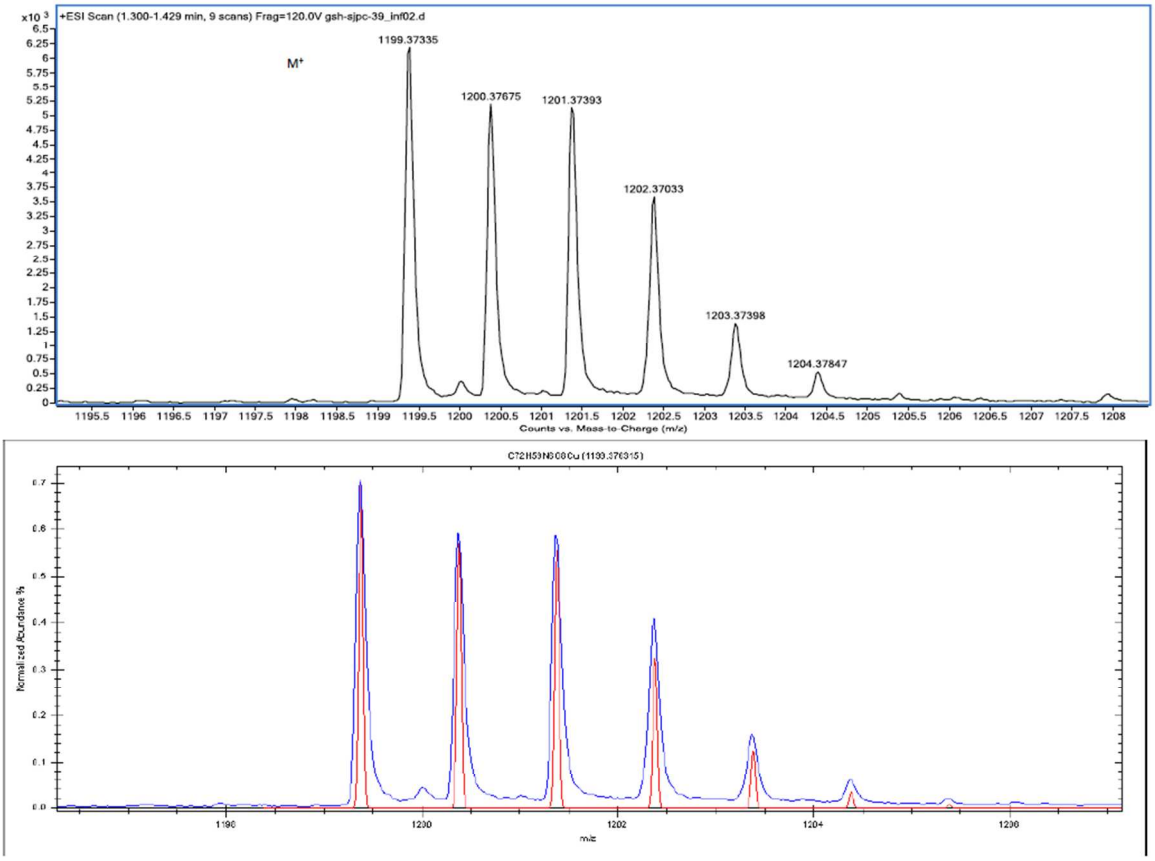

Figure S.4 – HR-ESIMS of compound **5b** and its fitting with theoretical spectrum.

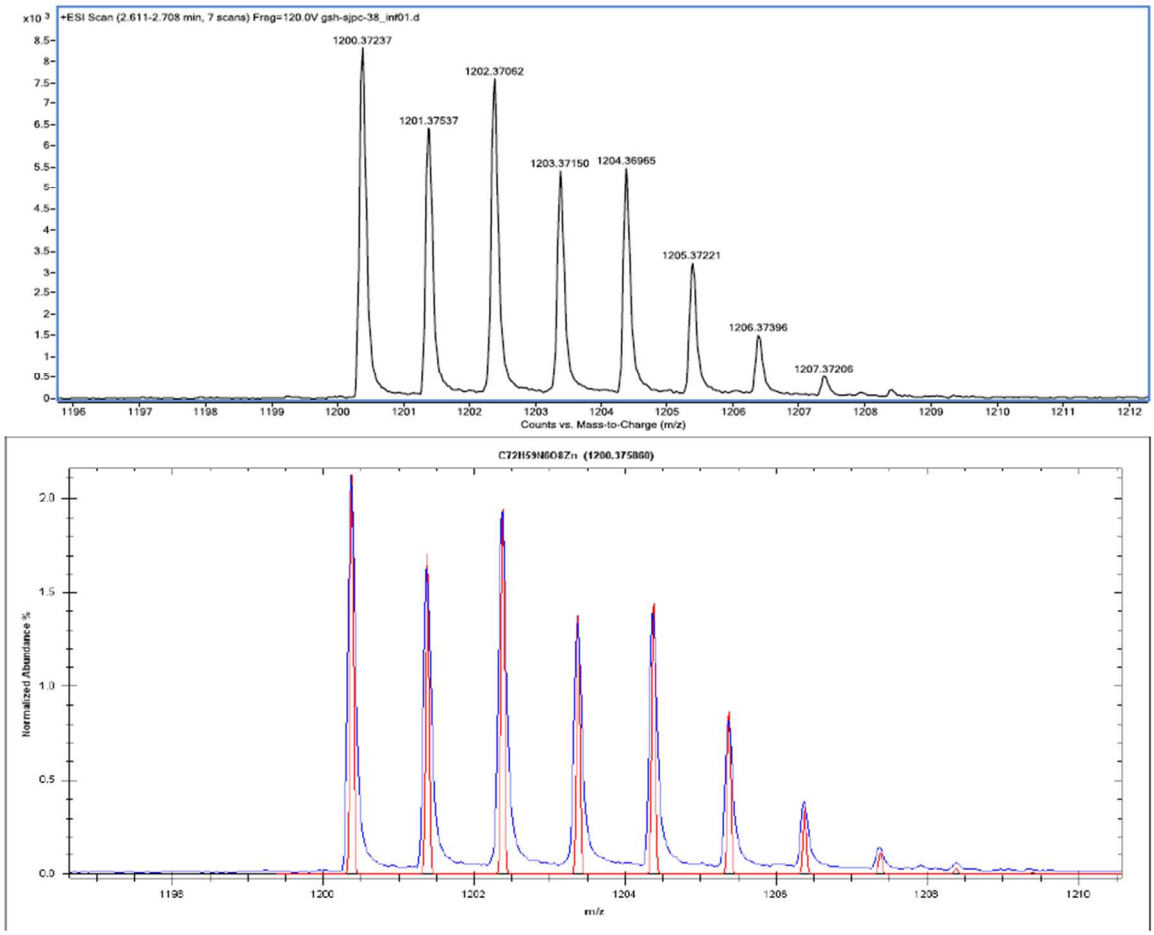

Figure S.5 – CV of ligand **1a** with ferrocene as internal reference.

(0.46V vs SCE in DCM) (Scan rate of 50 mV/s at R.T.)

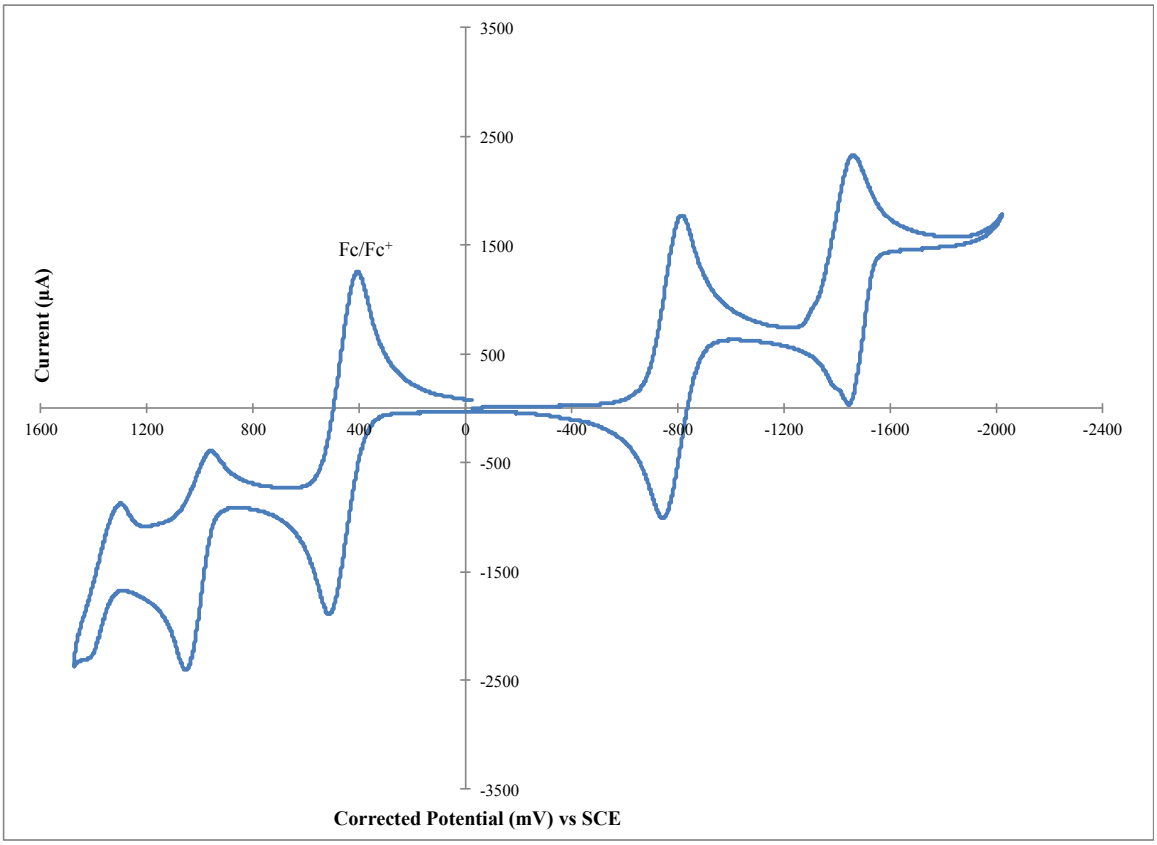

Figure S.6 – CV of ligand **1b** with ferrocene as internal reference.
(0.46V vs SCE in DCM) (Scan rate of 50 mV/s at R.T.)

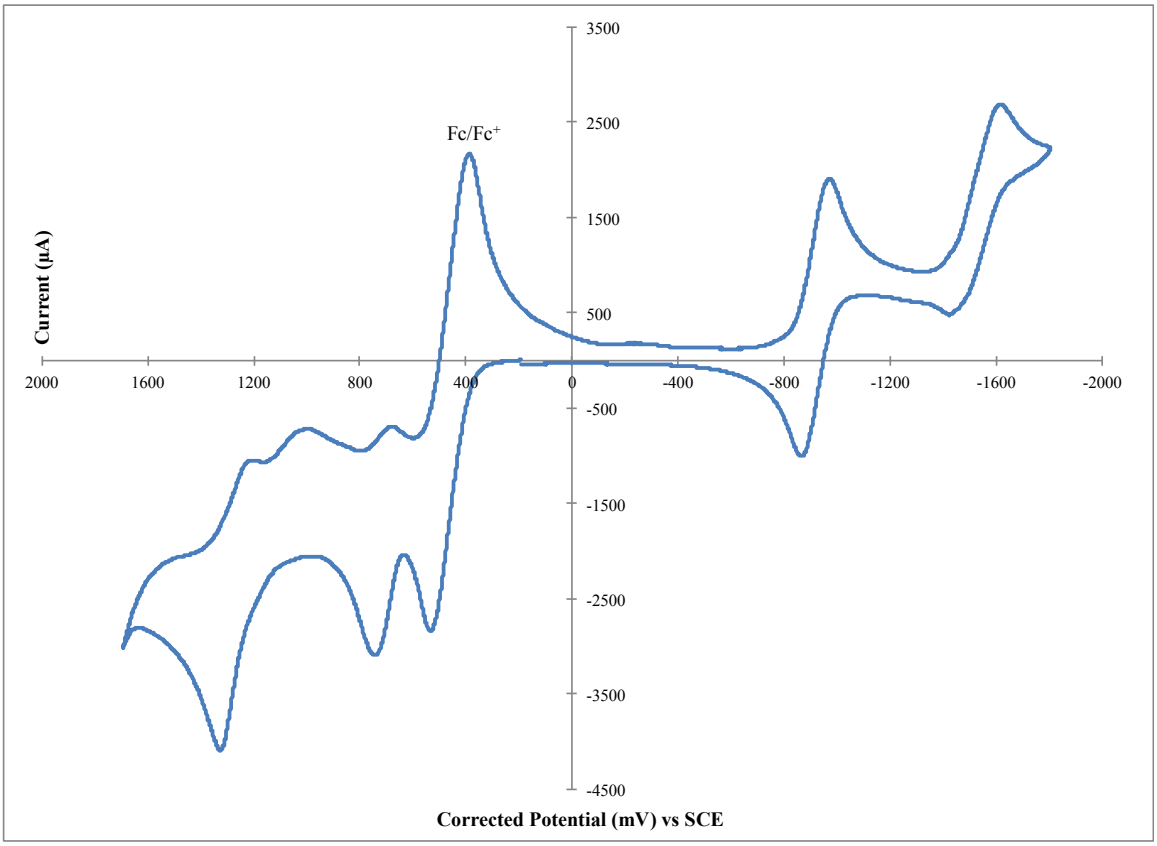

Figure S.7 – DPV of ligand **1b** with ferrocene as internal reference.

(0.46V vs SCE in DCM) (Scan rate of 50 mV/s at R.T.)

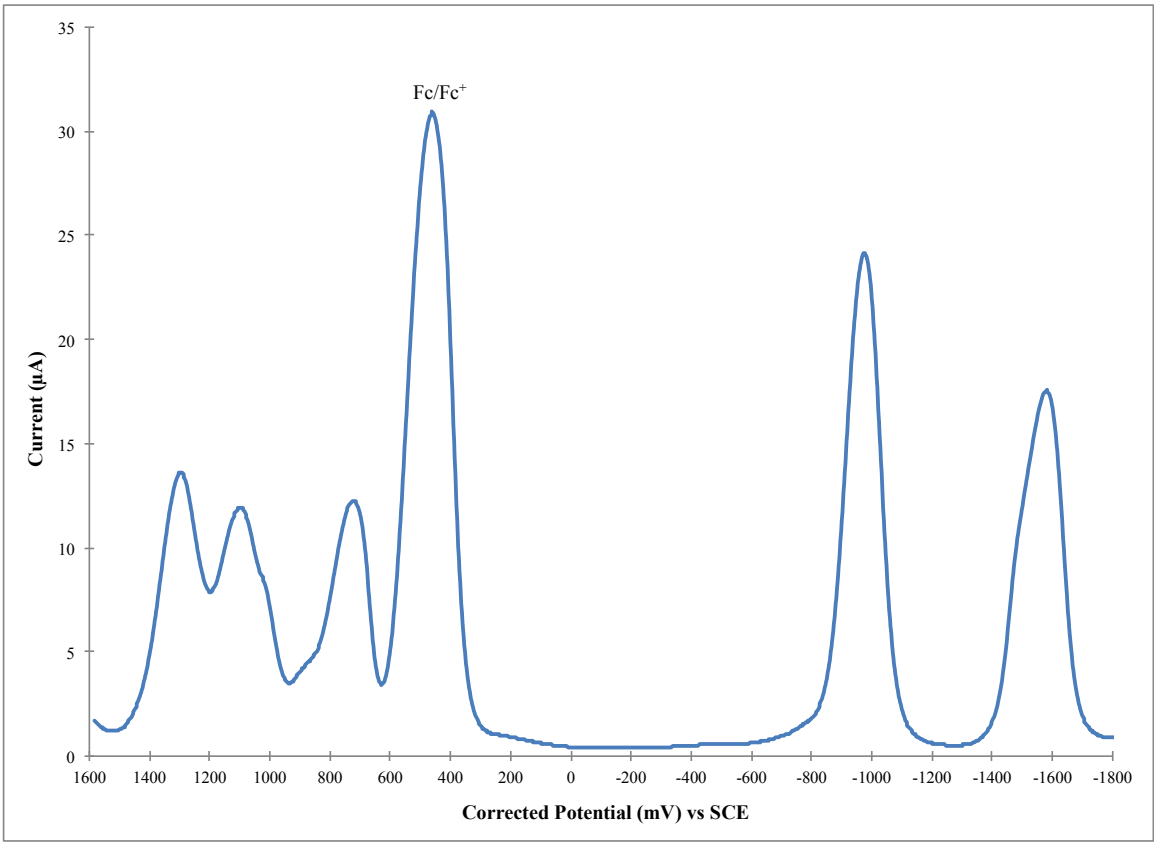

Figure S.8 – DPV of ligand **1b** before addition of ferrocene.

(Scan rate of 50 mV/s in DCM at R.T.)

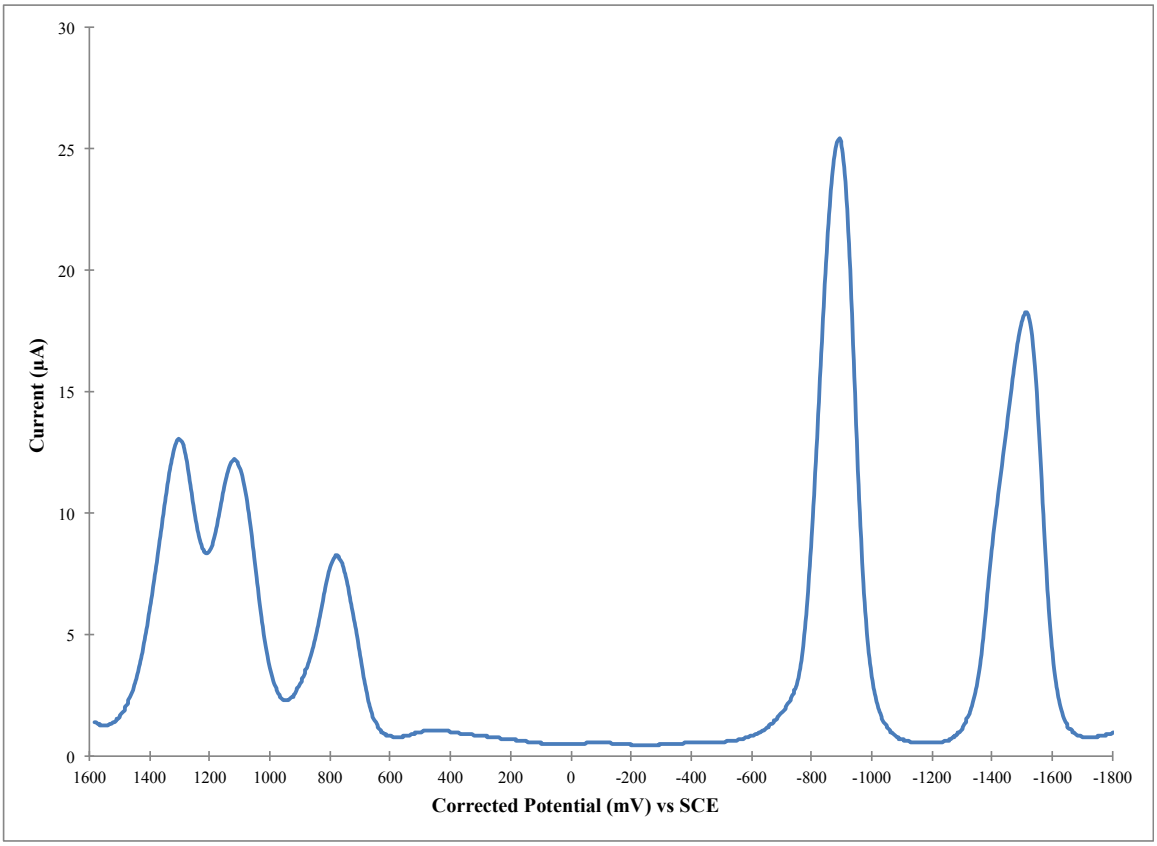

Figure S.9 – CV of Co(II) complex **2a** with ferrocene as internal reference.
(0.46V vs SCE in DCM) (Scan rate of 50 mV/s at R.T.)

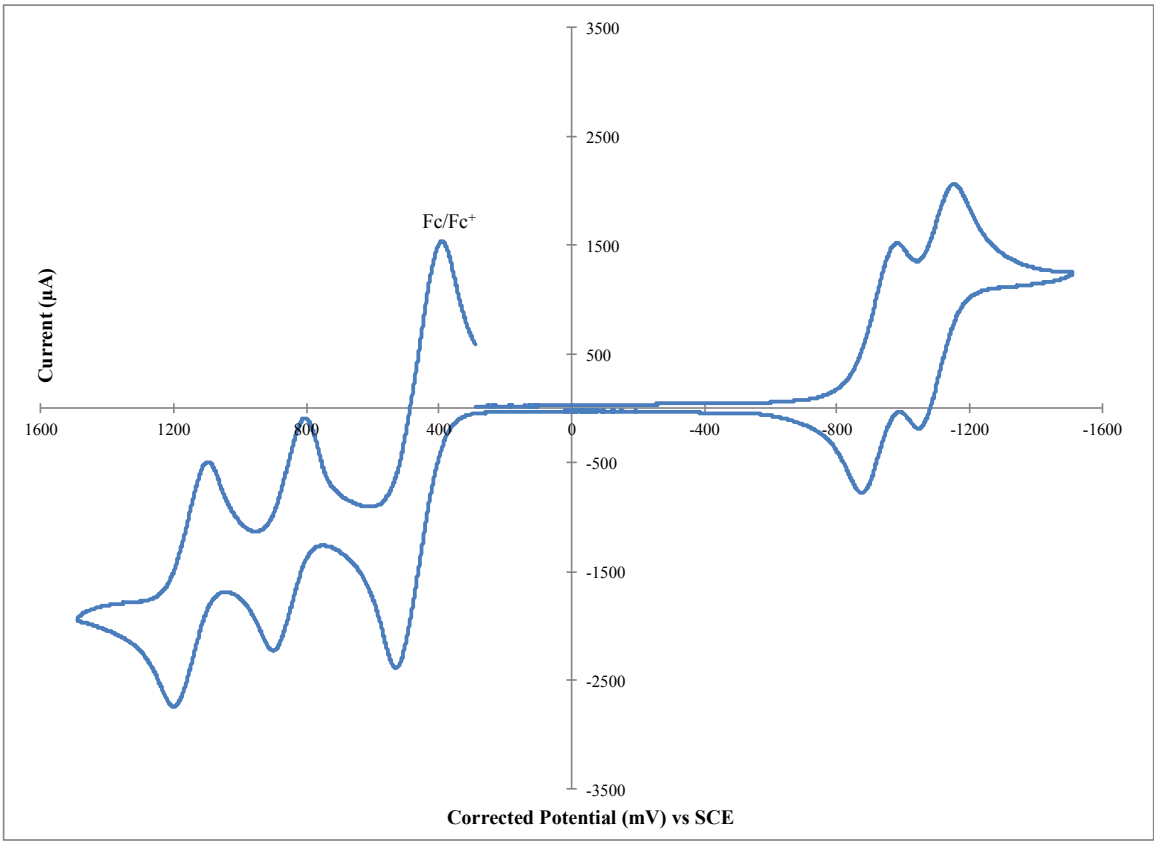

Figure S.10 – CV of Co(II) complex **2b** with ferrocene as internal reference (0.46V vs SCE in DCM) (Scan rate of 50 mV/s at R.T.)

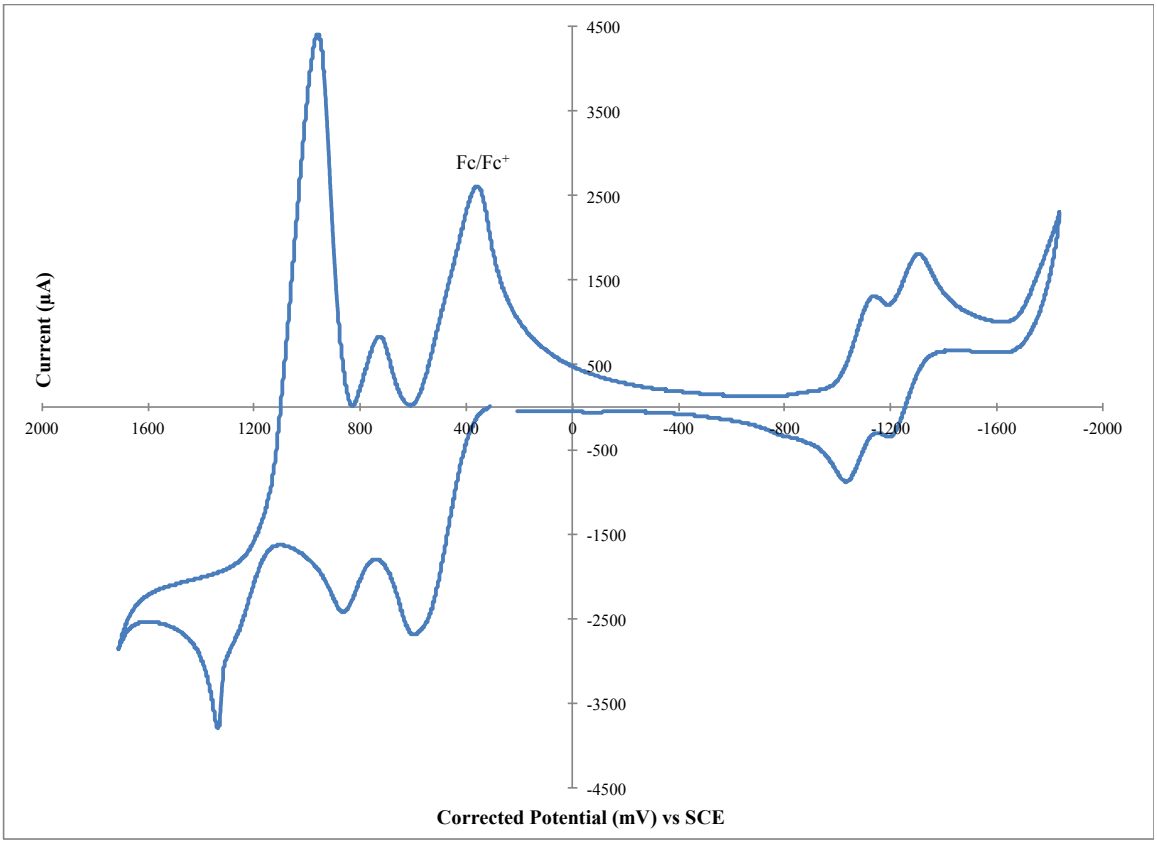

Figure S.11 – CV of Co(II) complex **2b** before addition of ferrocene.

(Scan rate of 50 mV/s in DCM at R.T.)

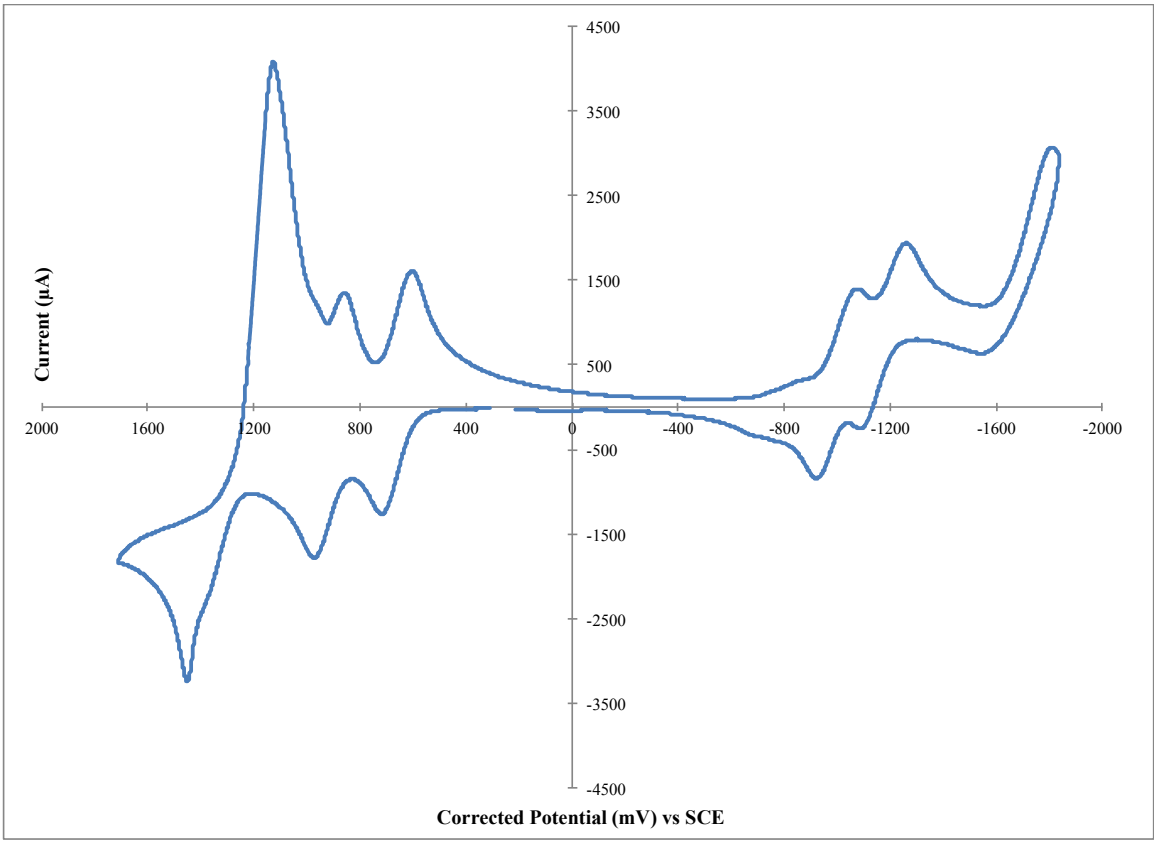

Figure S.12 – CV of Co(II) complex **2b** in the 2 firsts oxidation peaks region, showing the pseudo-reversible behavior.
(Scan rate of 50 mV/s in DCM at R.T. Before addition of ferrocene)

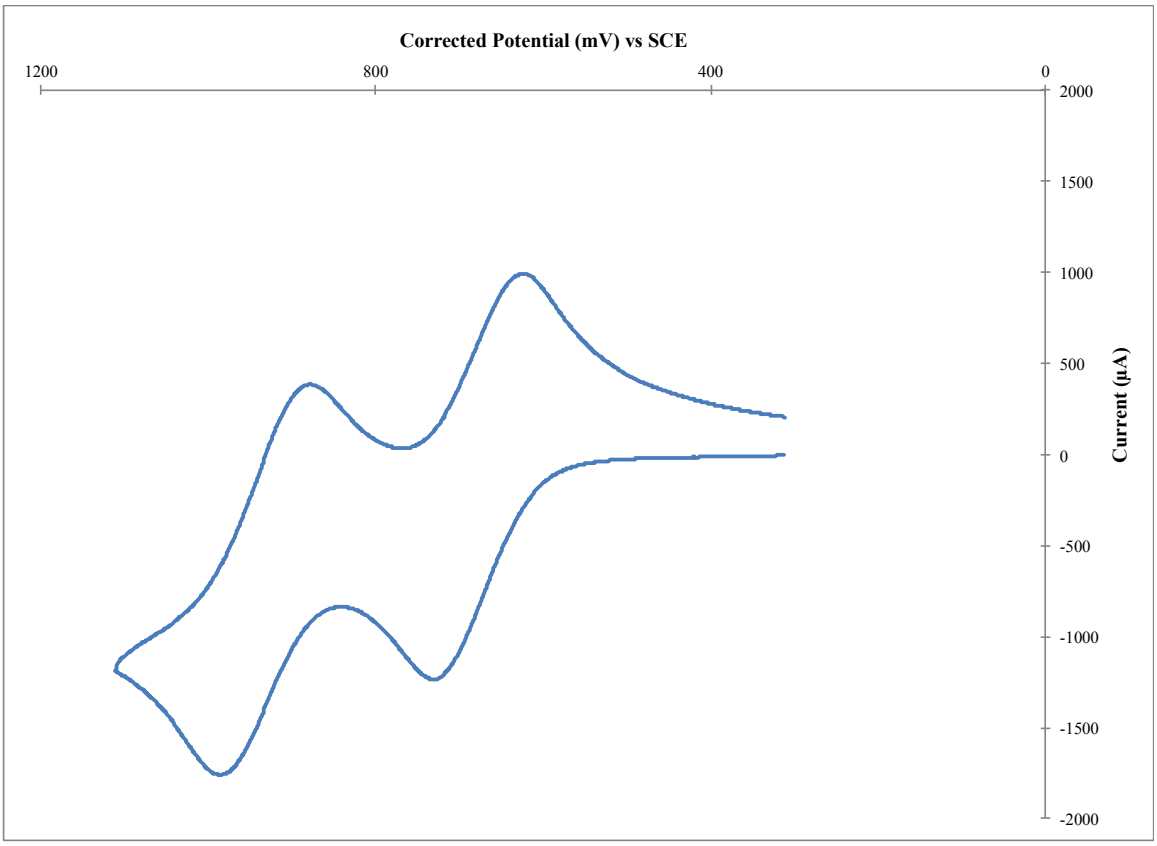

Figure S.13 – DPV of Co(II) complex **2b** with ferrocene as internal reference (0.46V vs SCE in DCM) (Scan rate of 50 mV/s at R.T.)

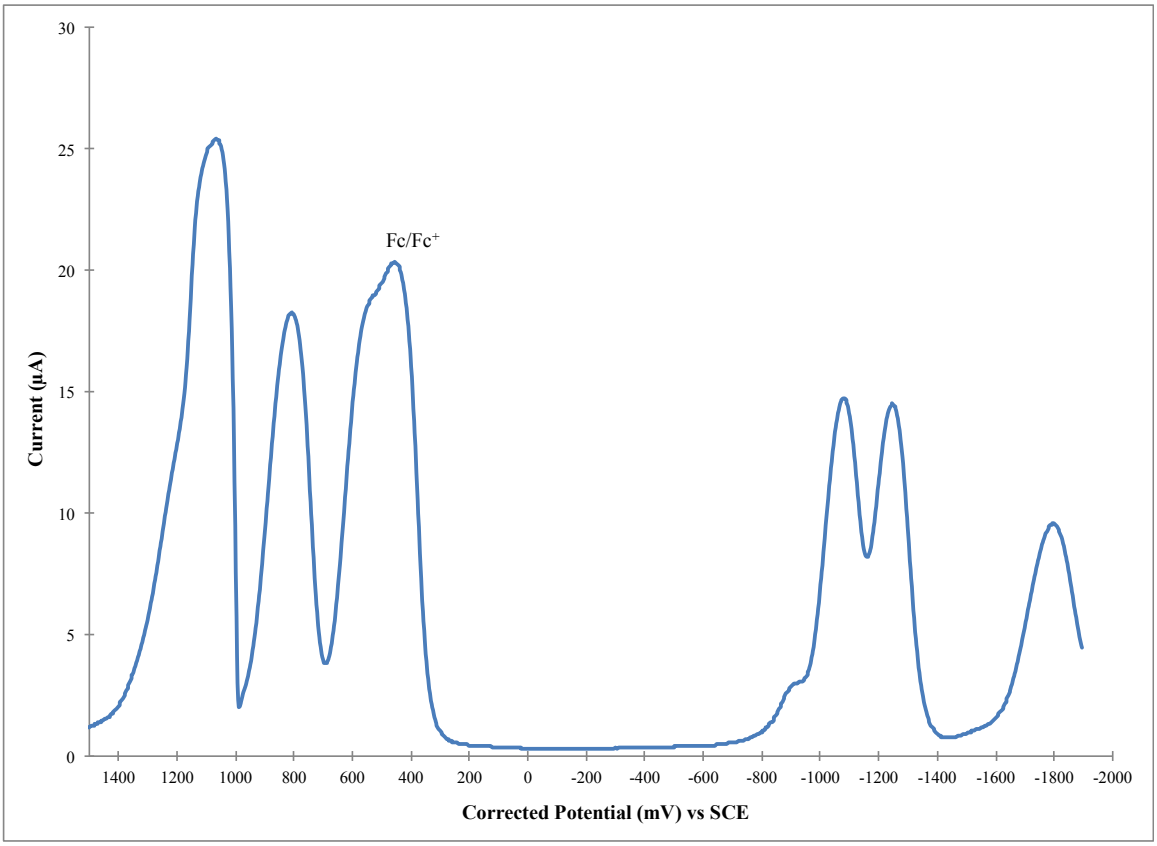

Figure S.14 – DPV of Co(II) complex **2b** with ferrocene as internal reference in the oxidation window only; showing the presence of 2 near oxidation peaks at 1.21 and 1.27 V . (0.46V vs SCE in DCM) (Scan rate of 50 mV/s at R.T.)

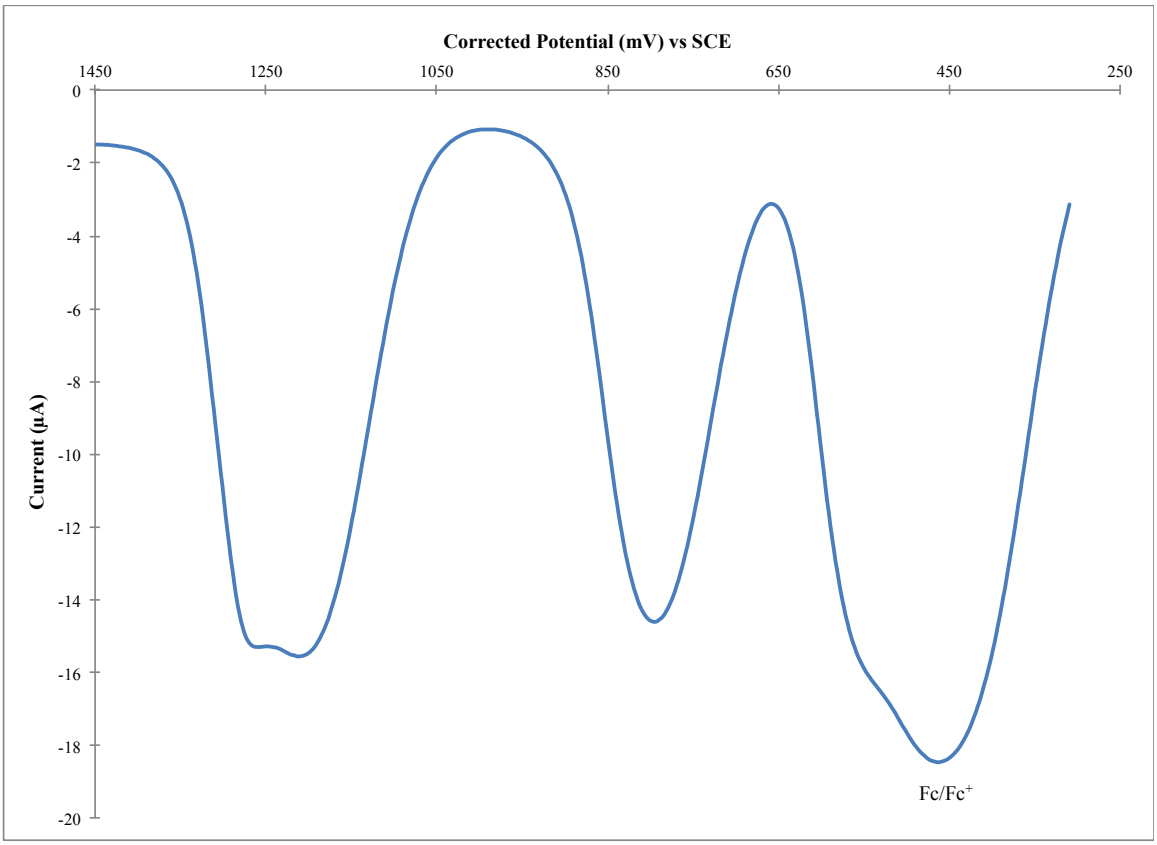

Figure S.15 – DPV of Co(II) complex **2b** before addition of ferrocene.

(Scan rate of 50 mV/s in DCM at R.T.)

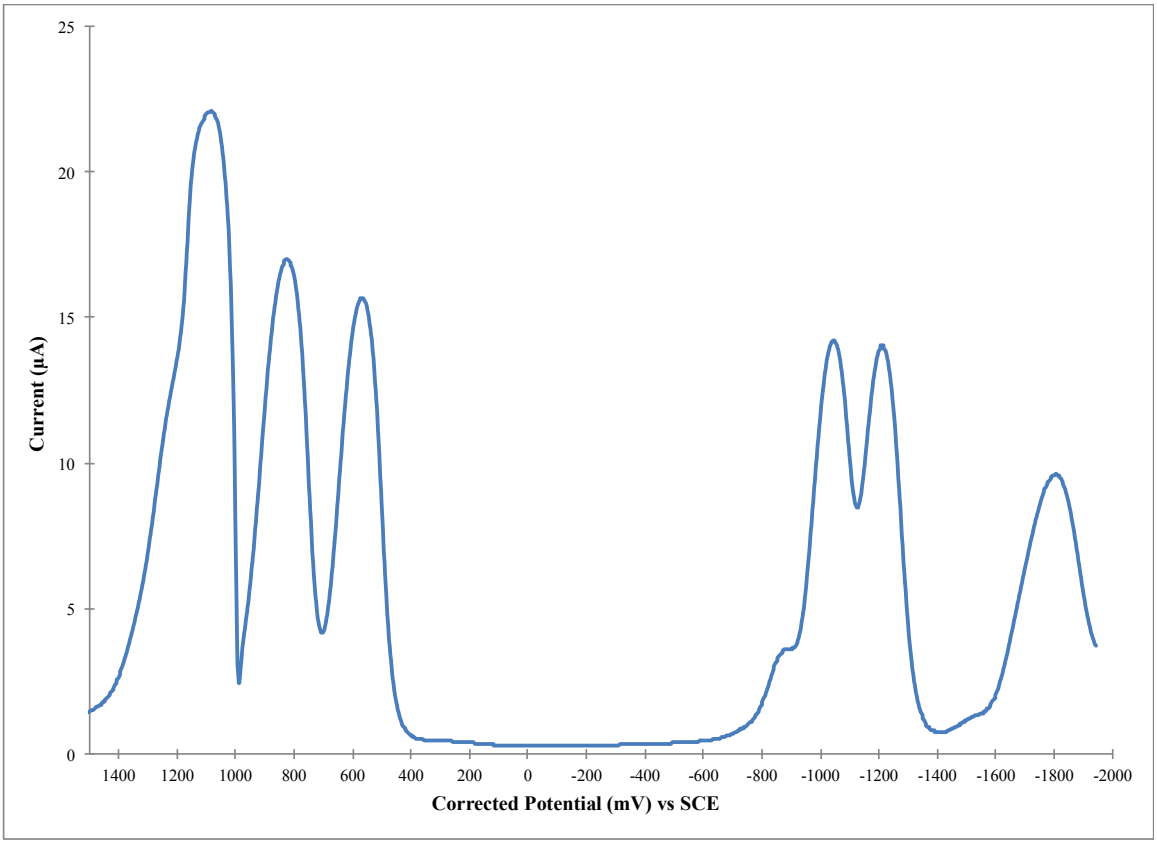

Figure S.16 – CV of Ni(II) complex **3a** with ferrocene as internal reference.
(0.46V vs SCE in DCM) (Scan rate of 50 mV/s at R.T.)

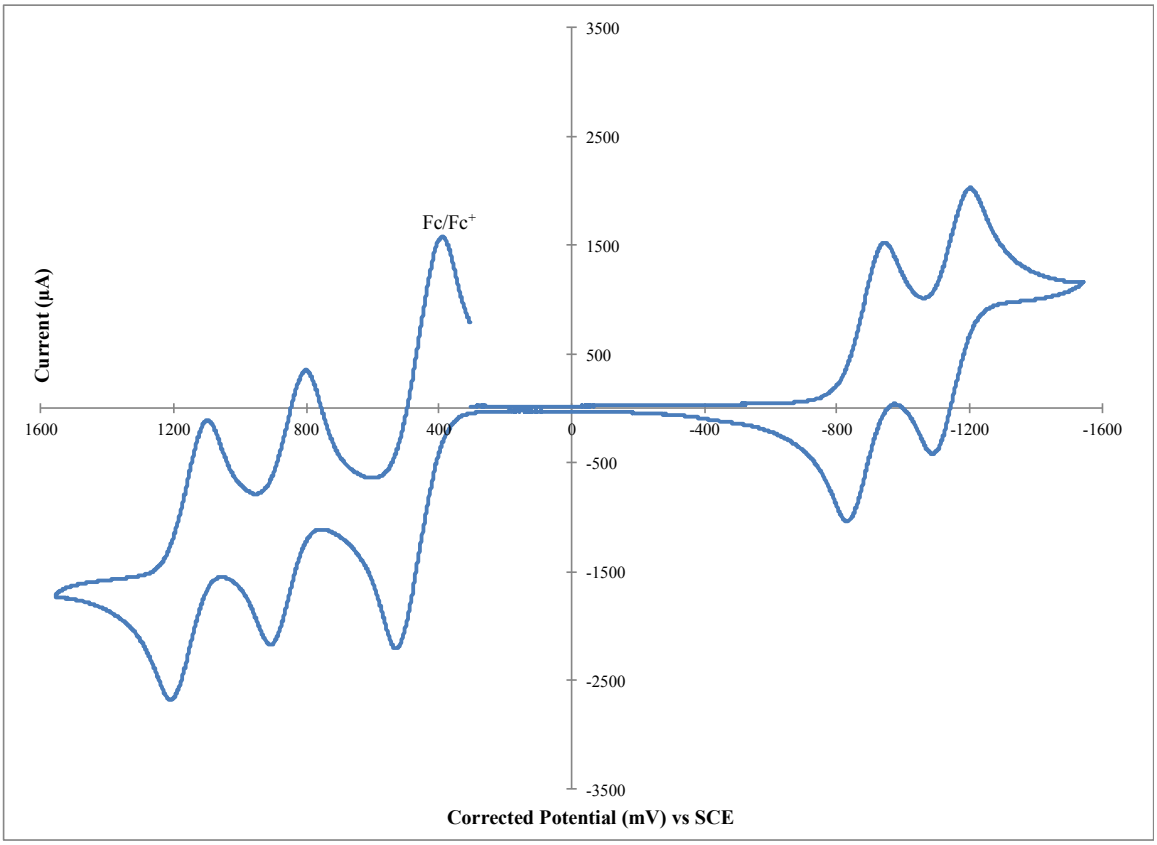

Figure S.17 – CV of Ni(II) complex **3b** with ferrocene as internal reference (0.46V vs SCE in DCM) (Scan rate of 50 mV/s at R.T.)

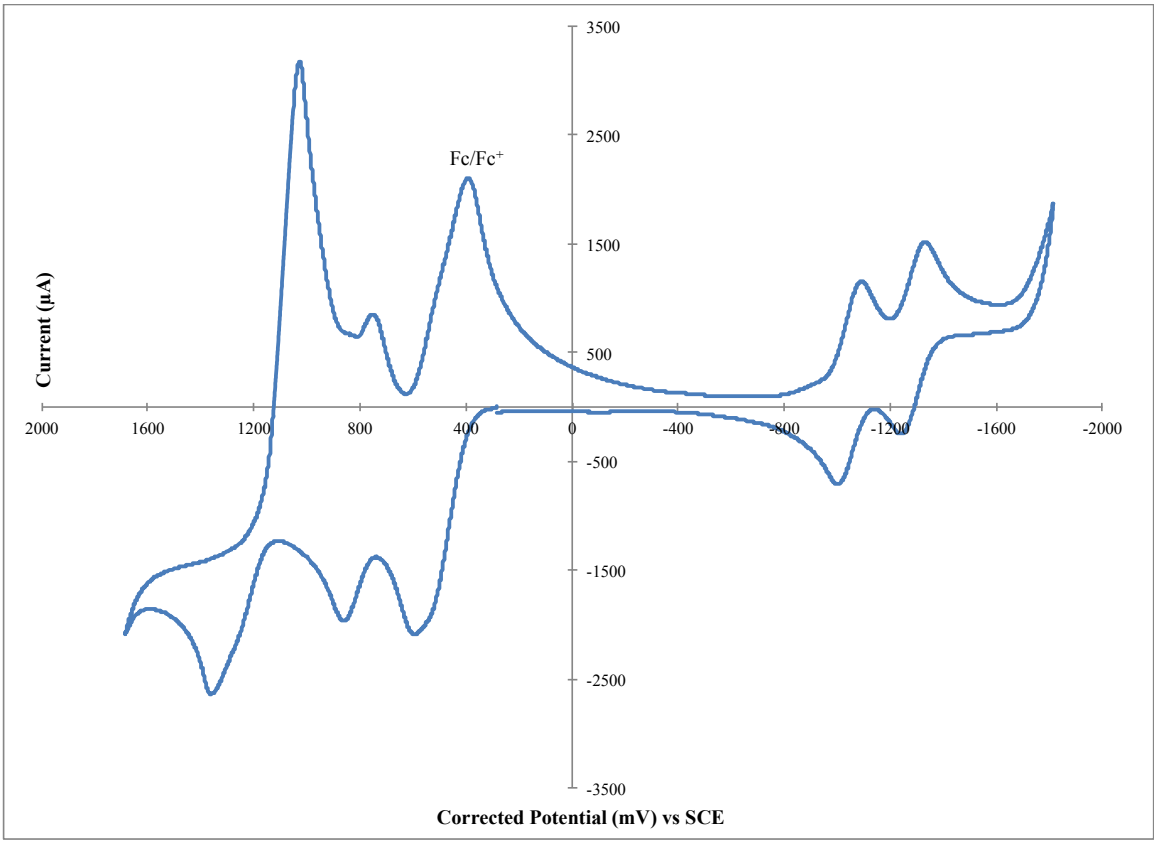

Figure S.18 – CV of Ni(II) complex **3b** before addition of ferrocene.

(Scan rate of 50 mV/s in DCM at R.T.)

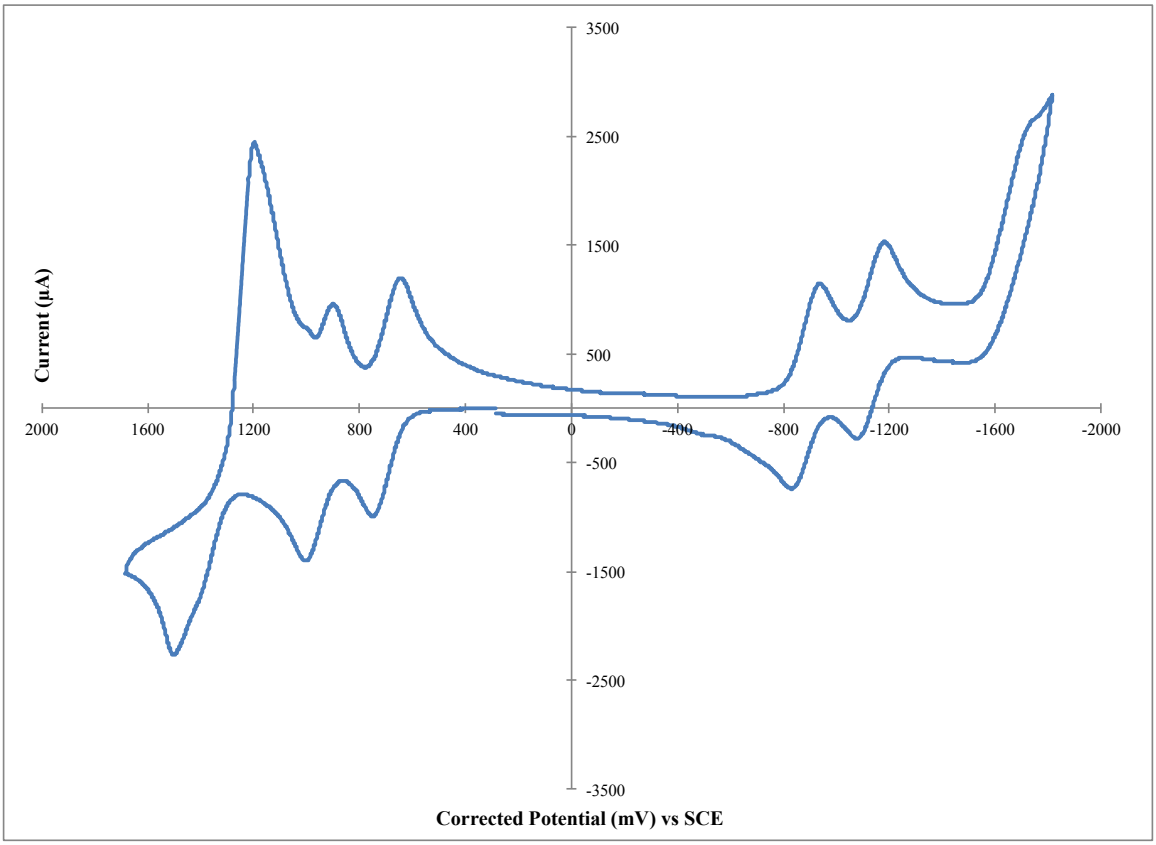

Figure S.19 – CV of Ni(II) complex **3b** in the potential region of the 2 firsts oxidation peaks, showing the pseudo-reversible behavior.
(Scan rate of 50 mV/s in DCM at R.T. Before addition of ferrocene)

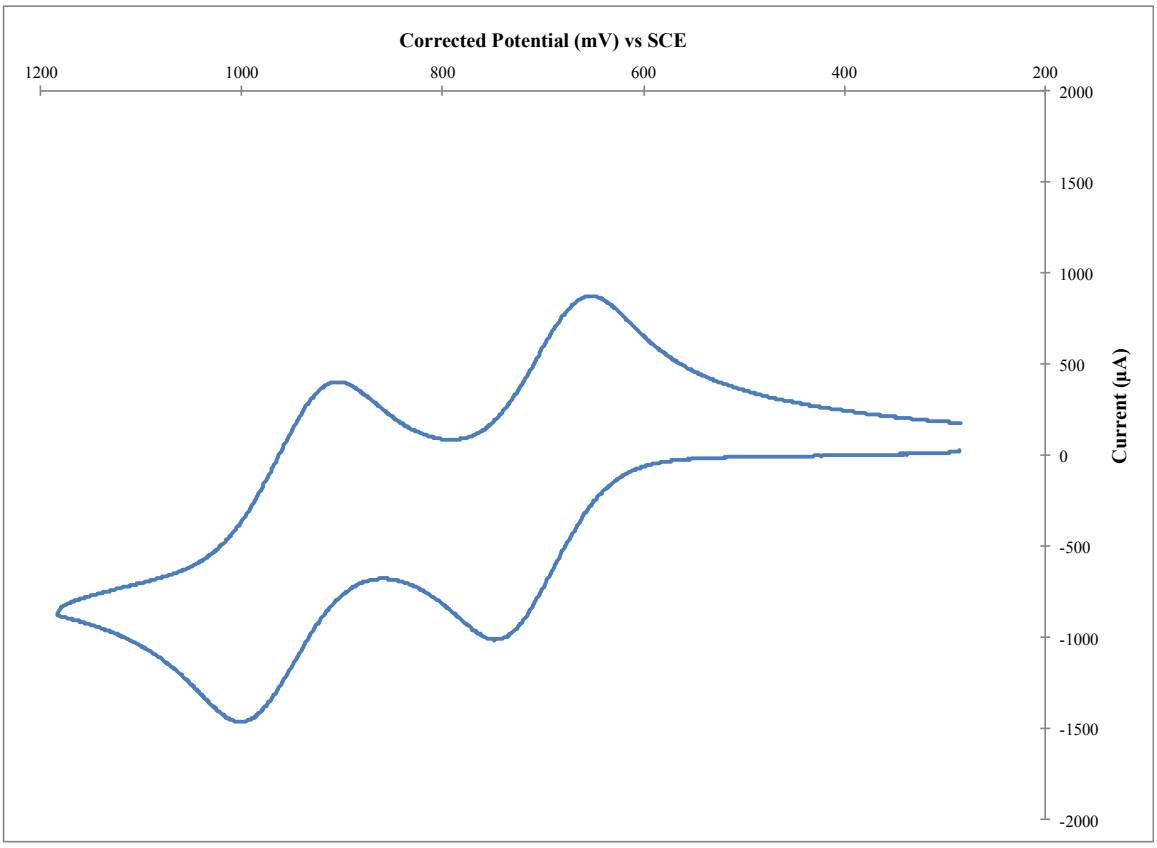

Figure S.20 – DPV of Ni(II) complex **3b** with ferrocene as internal reference (0.46V vs SCE in DCM) (Scan rate of 50 mV/s at R.T.)

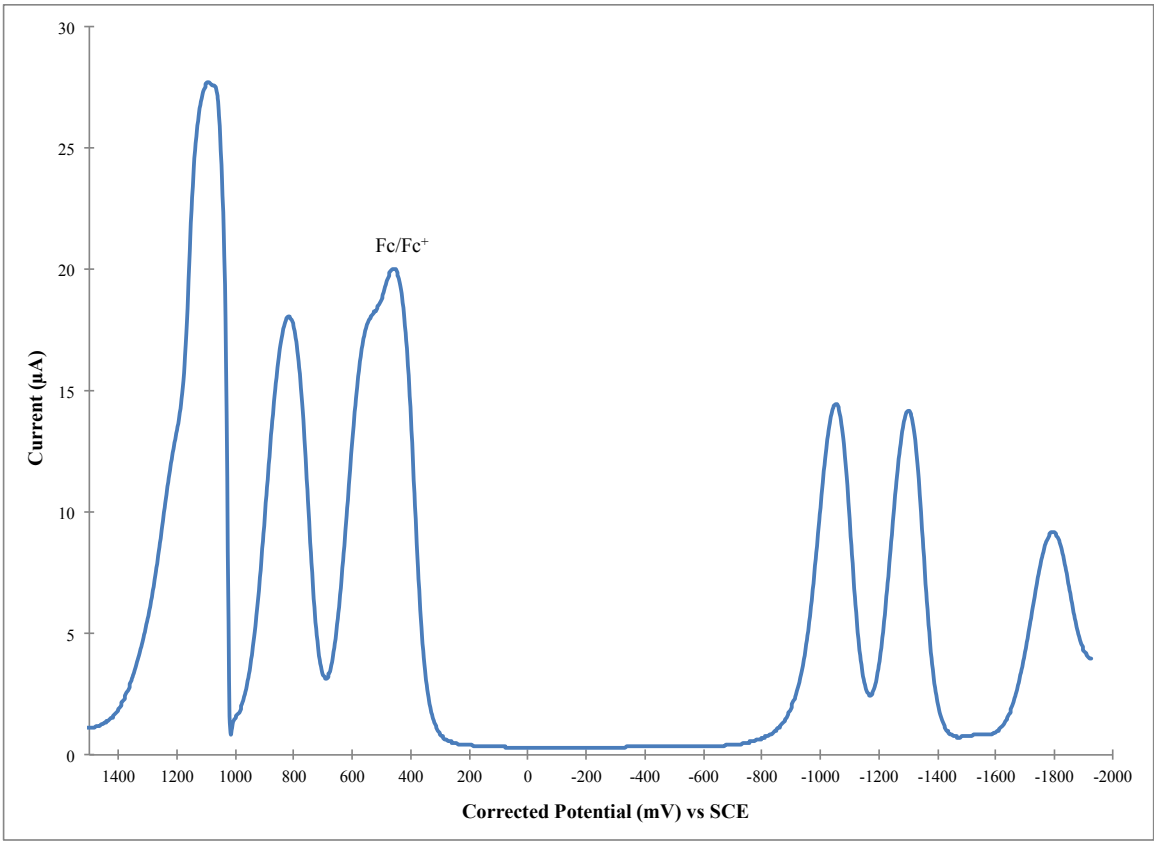

Figure S.21 – DPV of Ni(II) complex **3b** with ferrocene as internal reference in the oxidation window only; showing the presence of 2 near oxidation peaks at 1.21 and 1.28 V . (0.46V vs SCE in DCM) (Scan rate of 50 mV/s at R.T.)

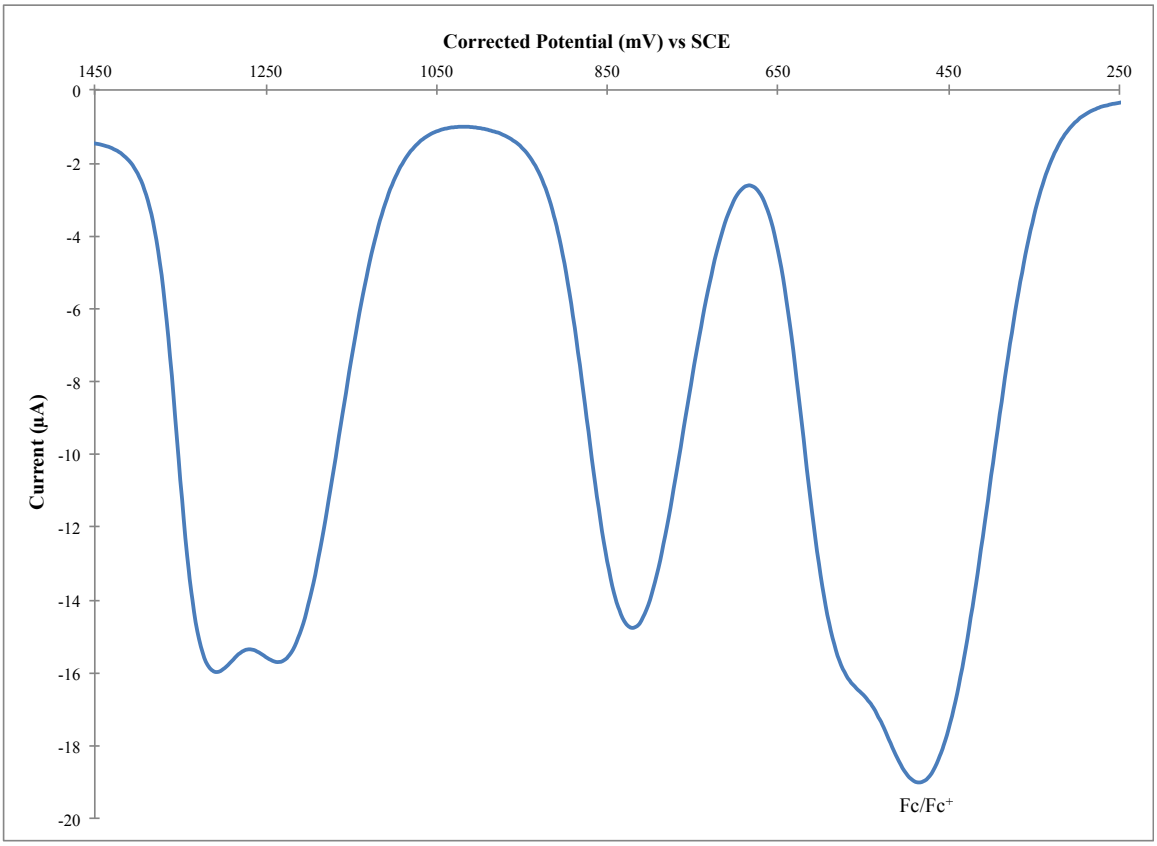

Figure S.22 – DPV of Ni(II) complex **3b** before addition of ferrocene.

(Scan rate of 50 mV/s in DCM at R.T.)

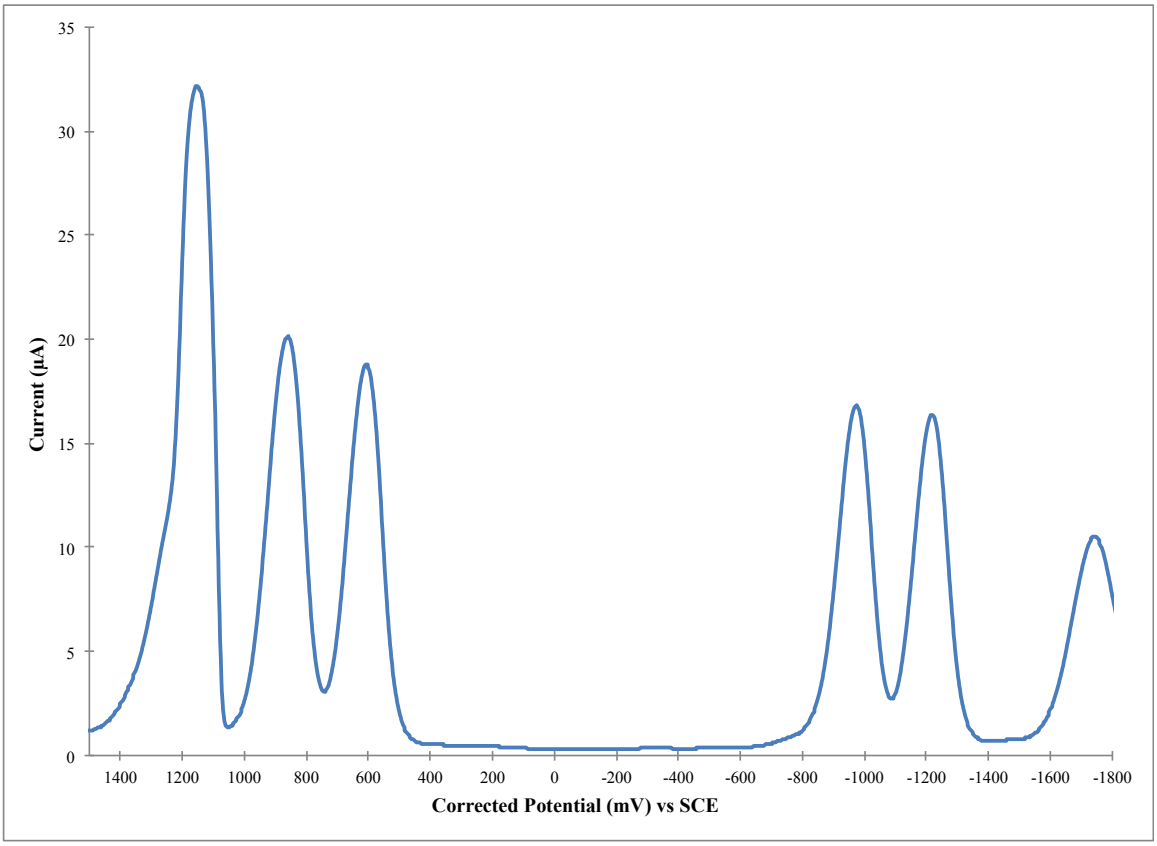

Figure S.23 – CV of Cu(II) complex **4a** with ferrocene as internal reference.
(0.46V vs SCE in DCM) (Scan rate of 50 mV/s at R.T.)

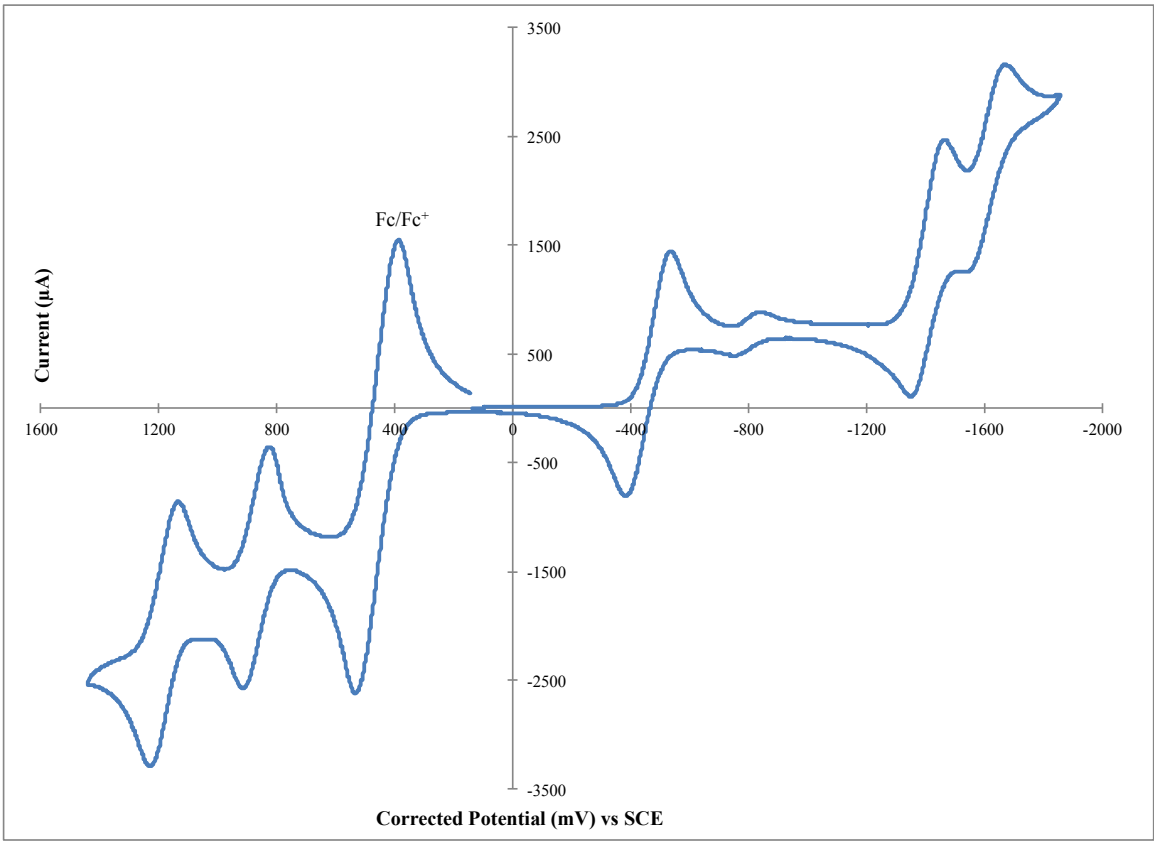

Figure S.24 – CV of Cu(II) complex **4b** with ferrocene as internal reference (0.46V vs SCE in DCM) (Scan rate of 50 mV/s at R.T.)

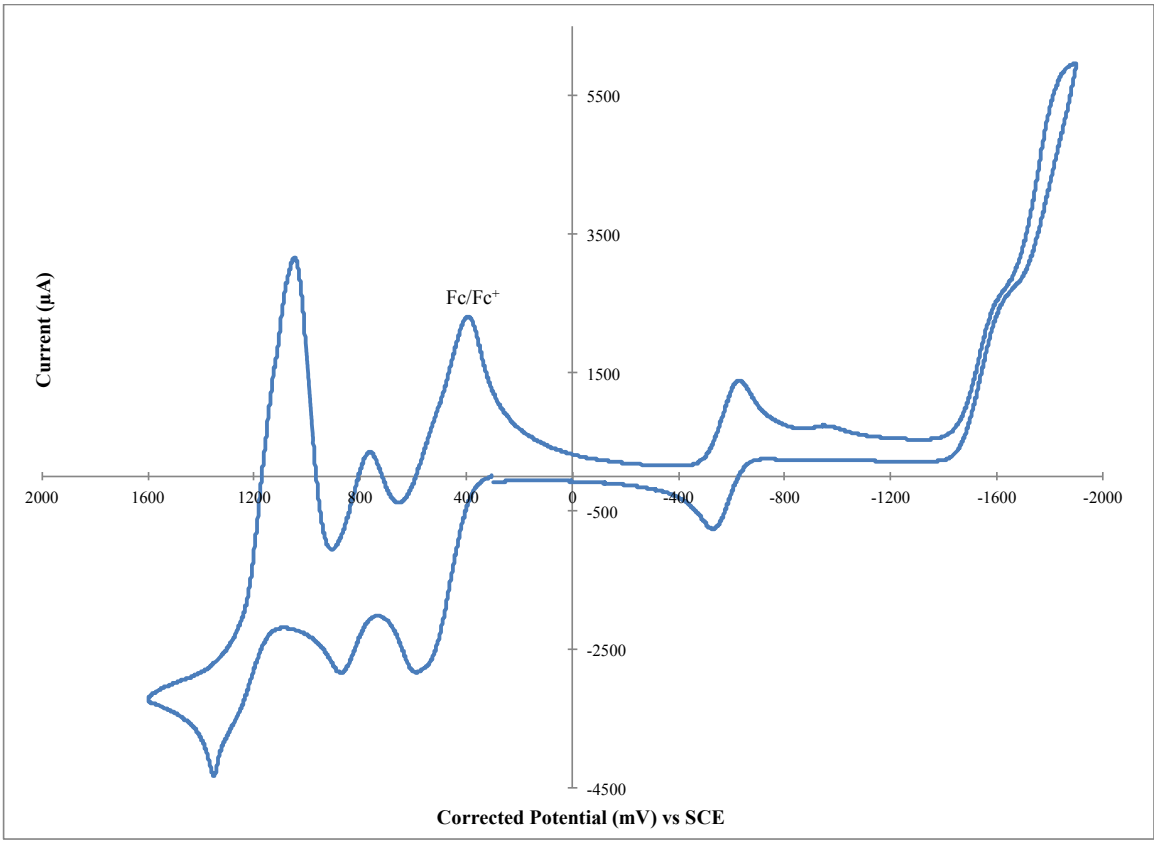

Figure S.25 – CV of Cu(II) complex **4b** before addition of ferrocene.

(Scan rate of 50 mV/s in DCM at R.T.)

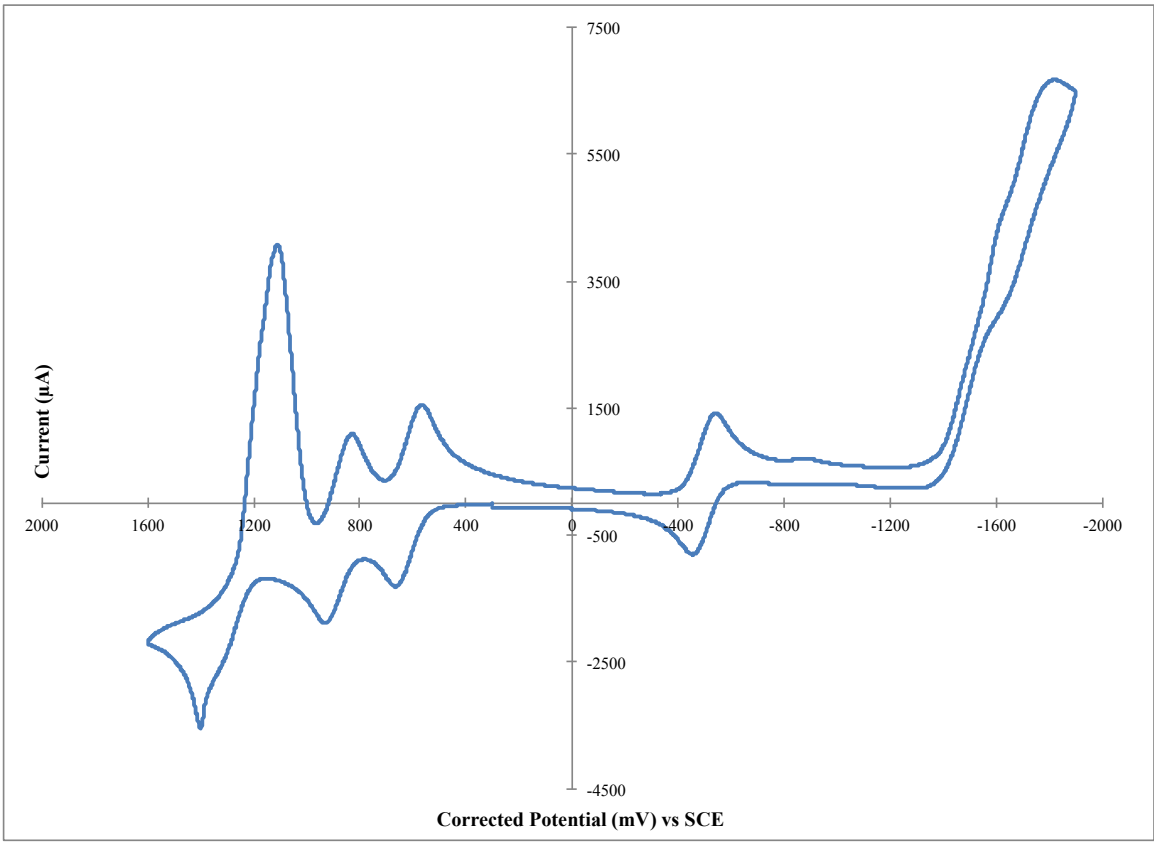

Figure S.26 – DPV of Cu(II) complex **4b** before addition of ferrocene in the oxidation window only; showing the presence of 2 near oxidation peaks at 1.19 and 1.25 V . (Scan rate of 50 mV/s at R.T.)

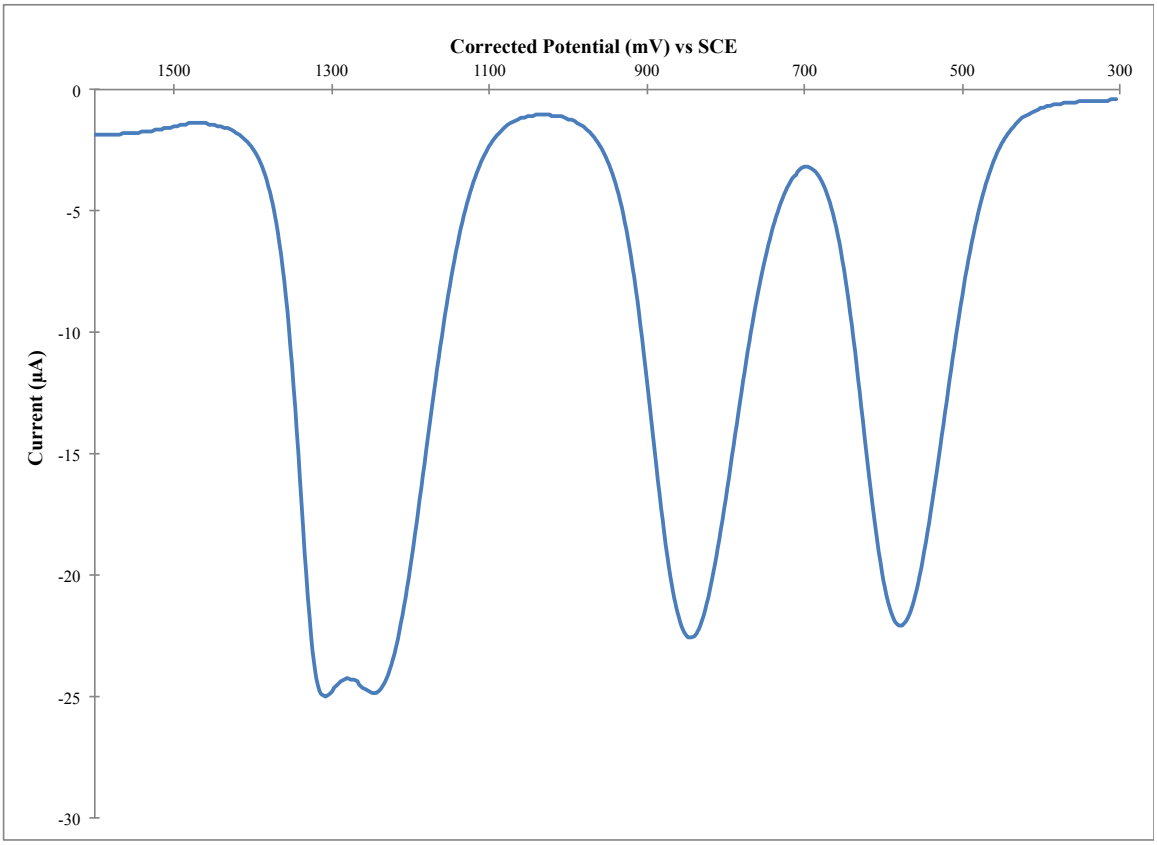

Figure S.27 – DPV of Cu(II) complex **4b** before addition of ferrocene in the reduction window only; (Scan rate of 50 mV/s at R.T.)

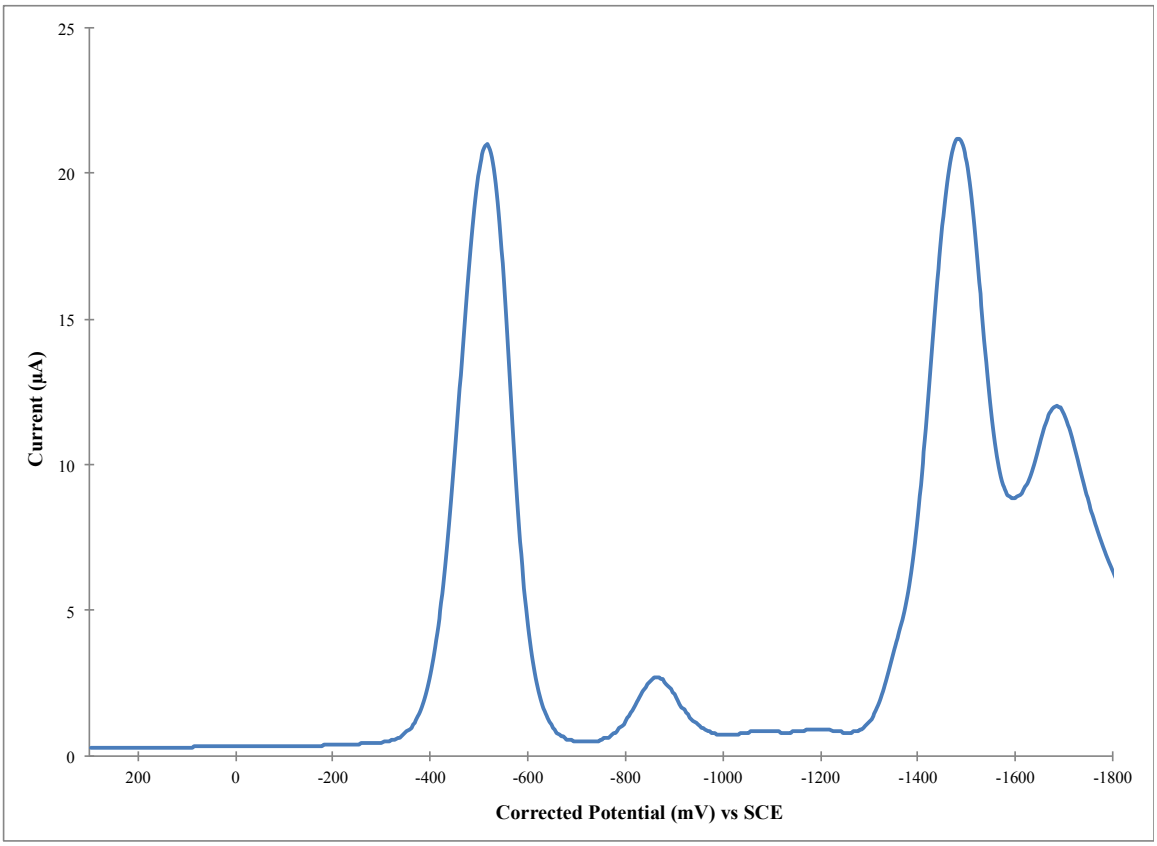

Figure S.28 – CV of Zn(II) complex **5a** with ferrocene as internal reference.
(0.46V vs SCE in DCM) (Scan rate of 50 mV/s at R.T.)

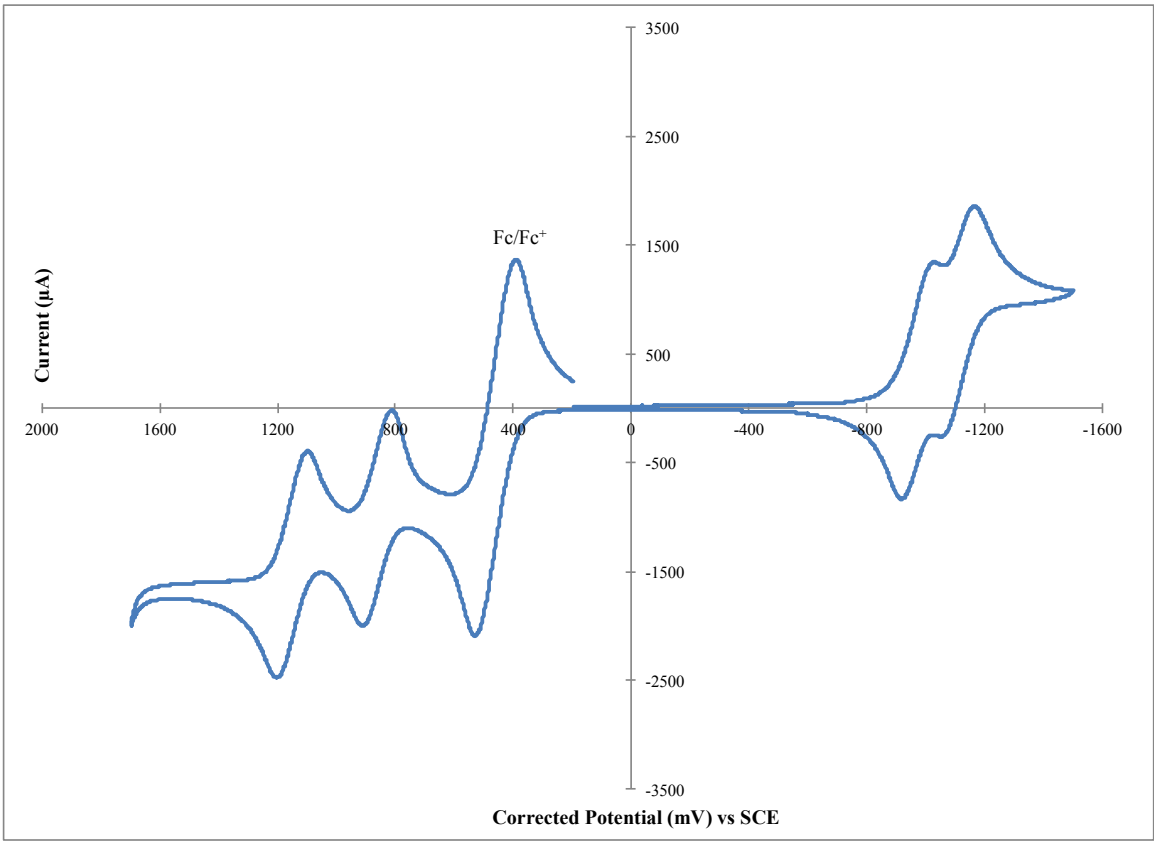

Figure S.29 – CV of Zn(II) complex **5b** with ferrocene as internal reference (0.46V vs SCE in DCM) (Scan rate of 50 mV/s at R.T.)

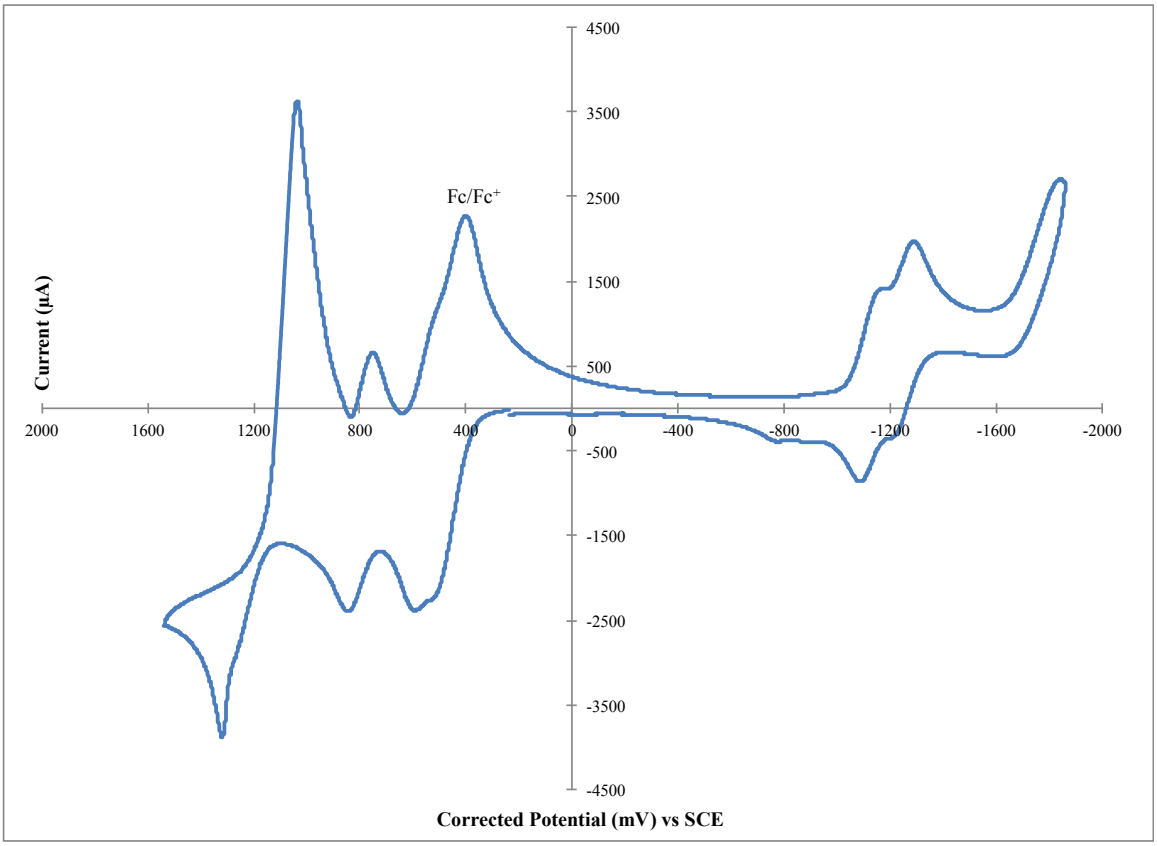

Figure S.30 – CV of Zn(II) complex **5b** before addition of ferrocene.

(Scan rate of 50 mV/s in DCM at R.T.)

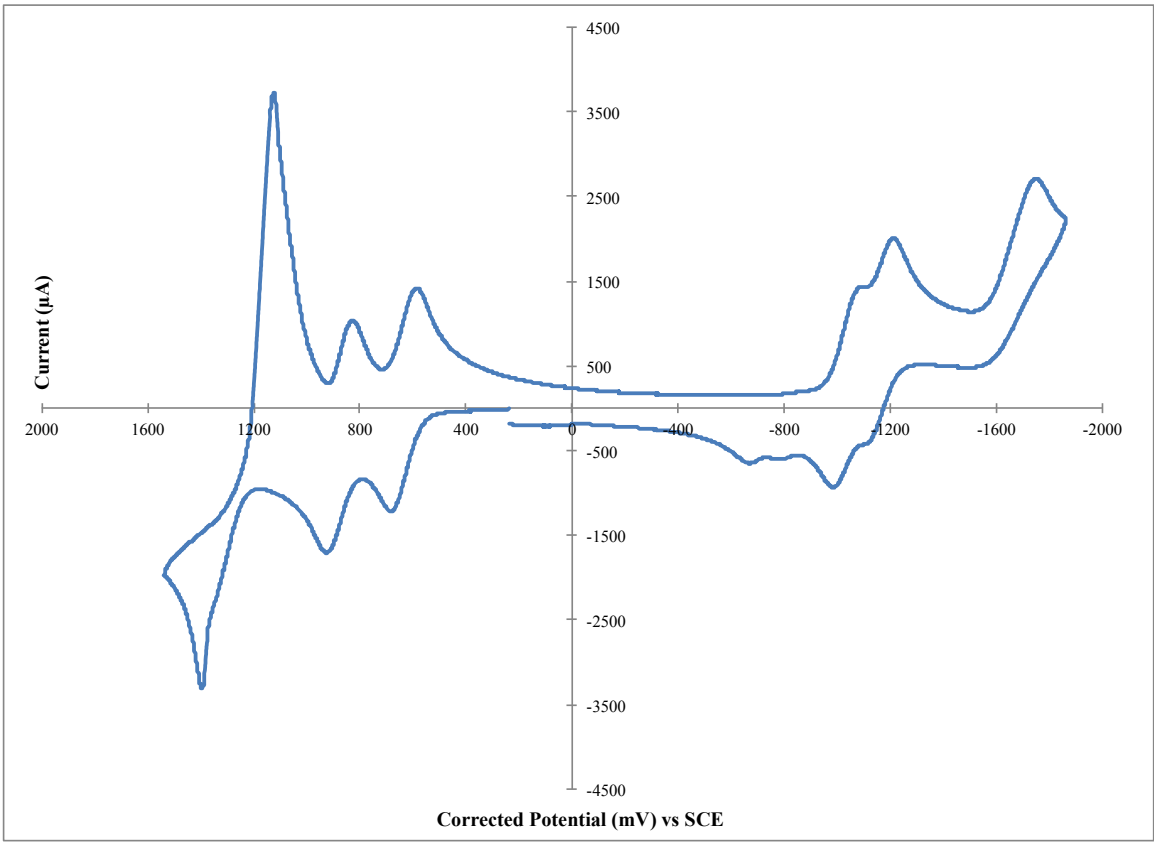

Figure S.31 – DPV of Zn(II) complex **5b** with ferrocene as internal reference (0.46V vs SCE in DCM) (Scan rate of 50 mV/s at R.T.)

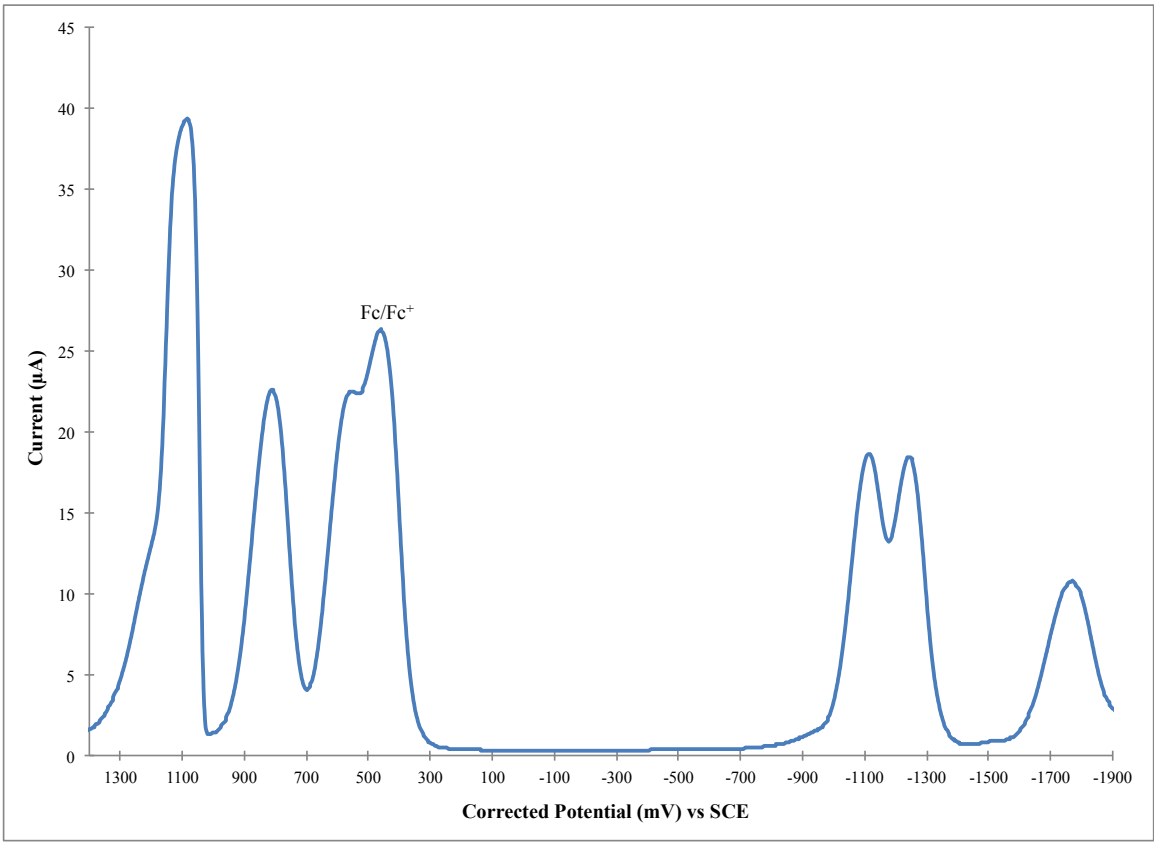

Figure S.32 – DPV of Zn(II) complex **5b** with ferrocene as internal reference in the oxidation window only; showing the presence of 2 near oxidation peaks at 1.22 and 1.25 V . (0.46V vs SCE in DCM) (Scan rate of 50 mV/s at R.T.)

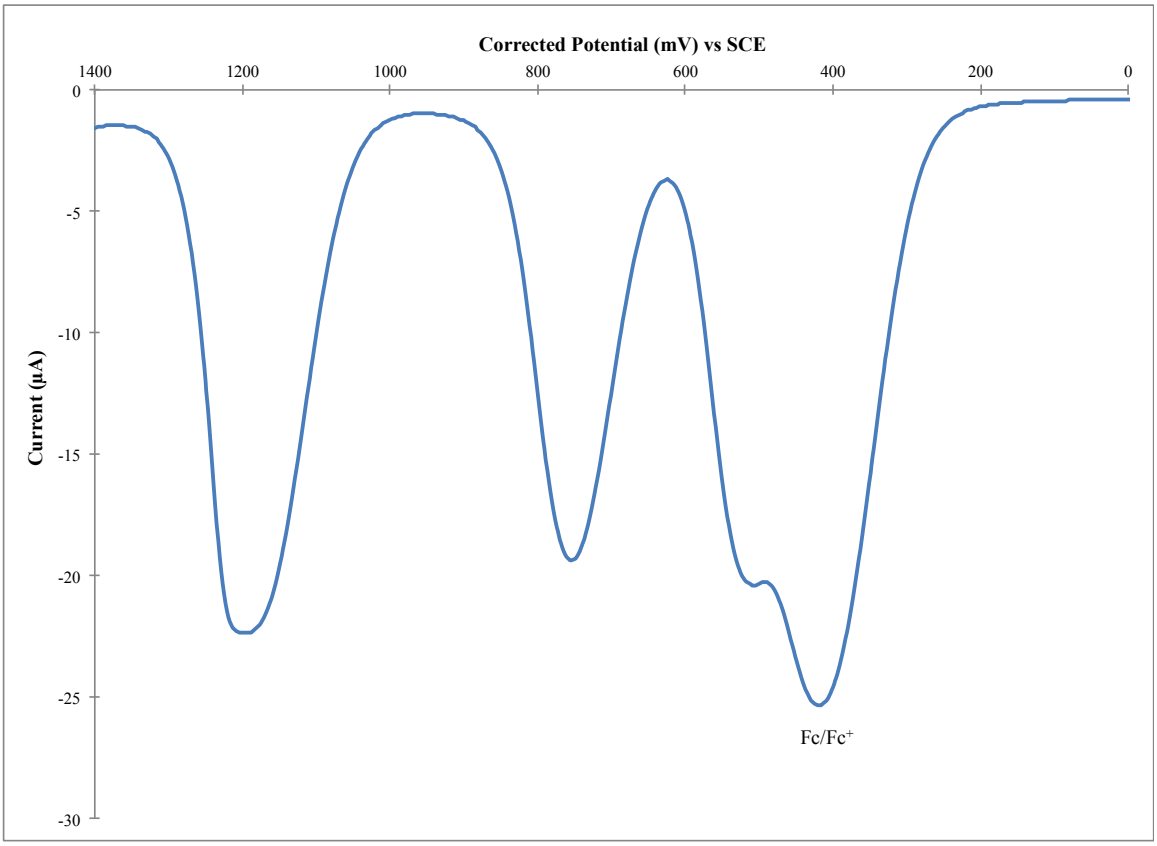

Figure S.33 – DPV of Zn(II) complex **5b** before addition of ferrocene.

(Scan rate of 50 mV/s in DCM at R.T.)

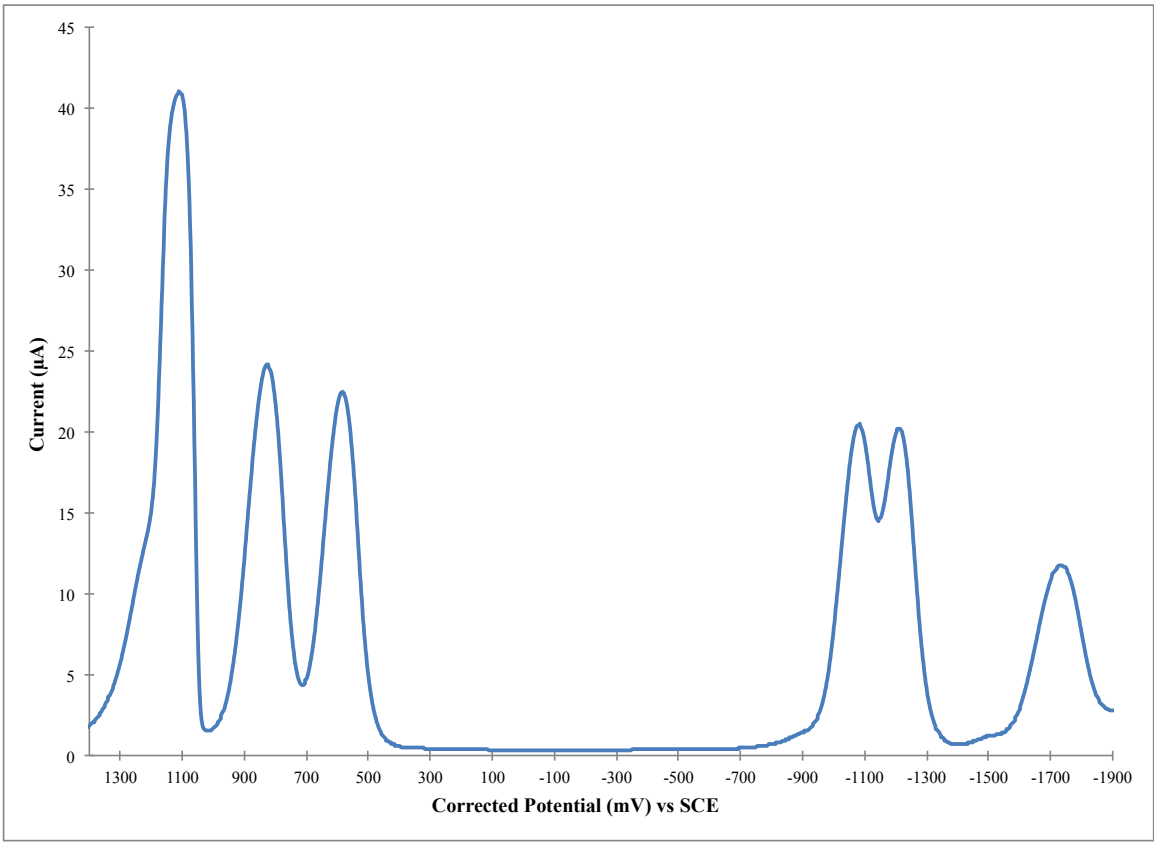

Figure S.34 – CV of Aza-BODIPY complex **6a** with ferrocene as internal reference (0.46V vs SCE in DCM). (Scan rate of 50 mV/s at R.T.)

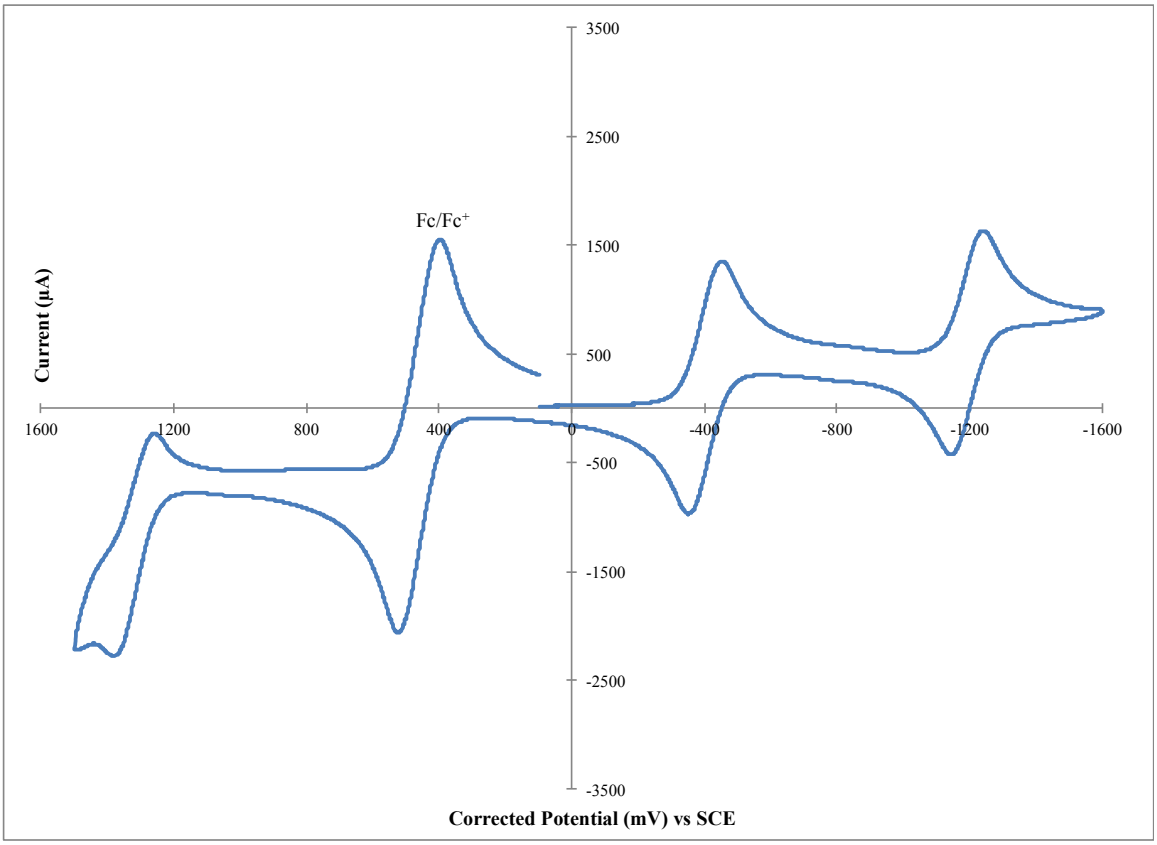

Figure S.35 – DPV of Aza-BODIPY complex **6a** with ferrocene as internal reference (0.46V vs SCE in DCM). (Scan rate of 50 mV/s at R.T.)

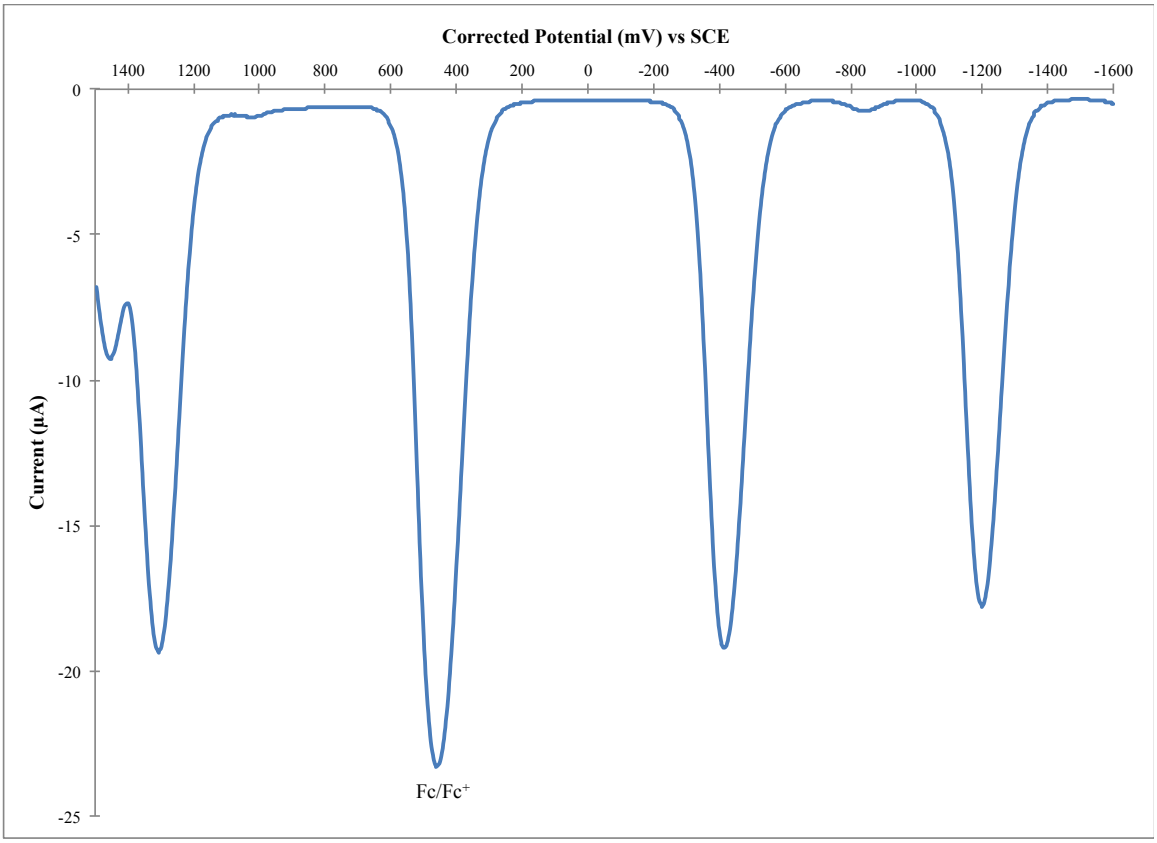

Figure S.36 – CV of Aza-BODIPY complex **6b** with ferrocene as internal reference (0.46V vs SCE in DCM). (Scan rate of 50 mV/s at R.T.)

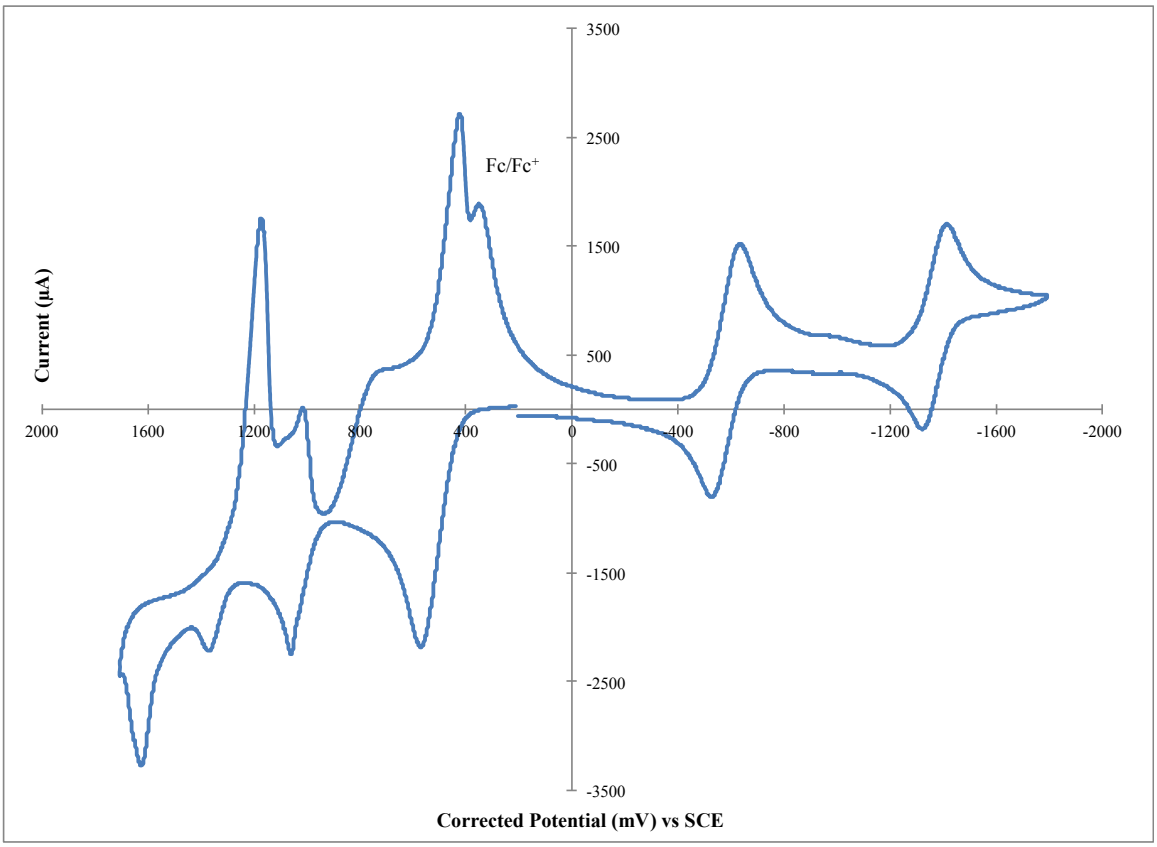

Figure S.37 – DPV of Aza-BODIPY complex **6b** with ferrocene as internal reference (0.46V vs SCE in DCM). (Scan rate of 50 mV/s at R.T.)

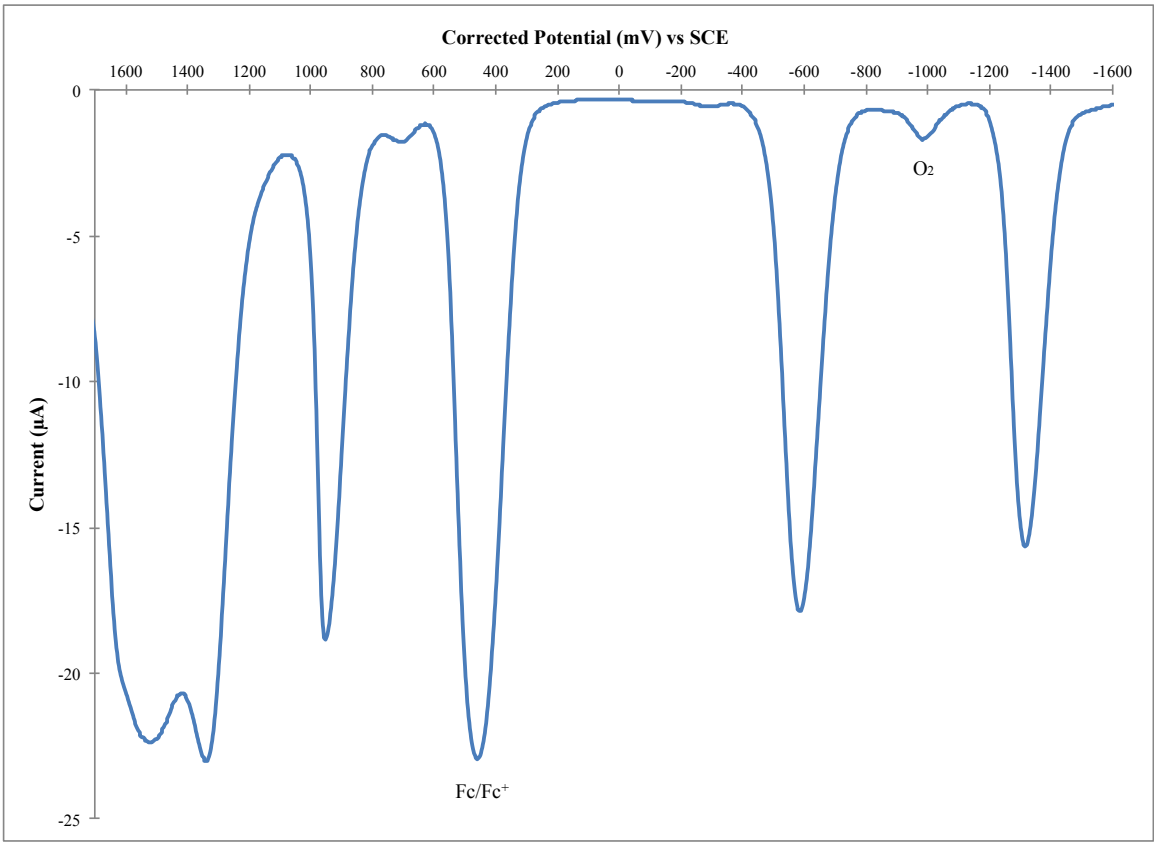

Figure S.38 – DPV of Aza-BODIPY complex **6b** before addition of ferrocene.

(Scan rate of 50 mV/s in DCM at R.T.)

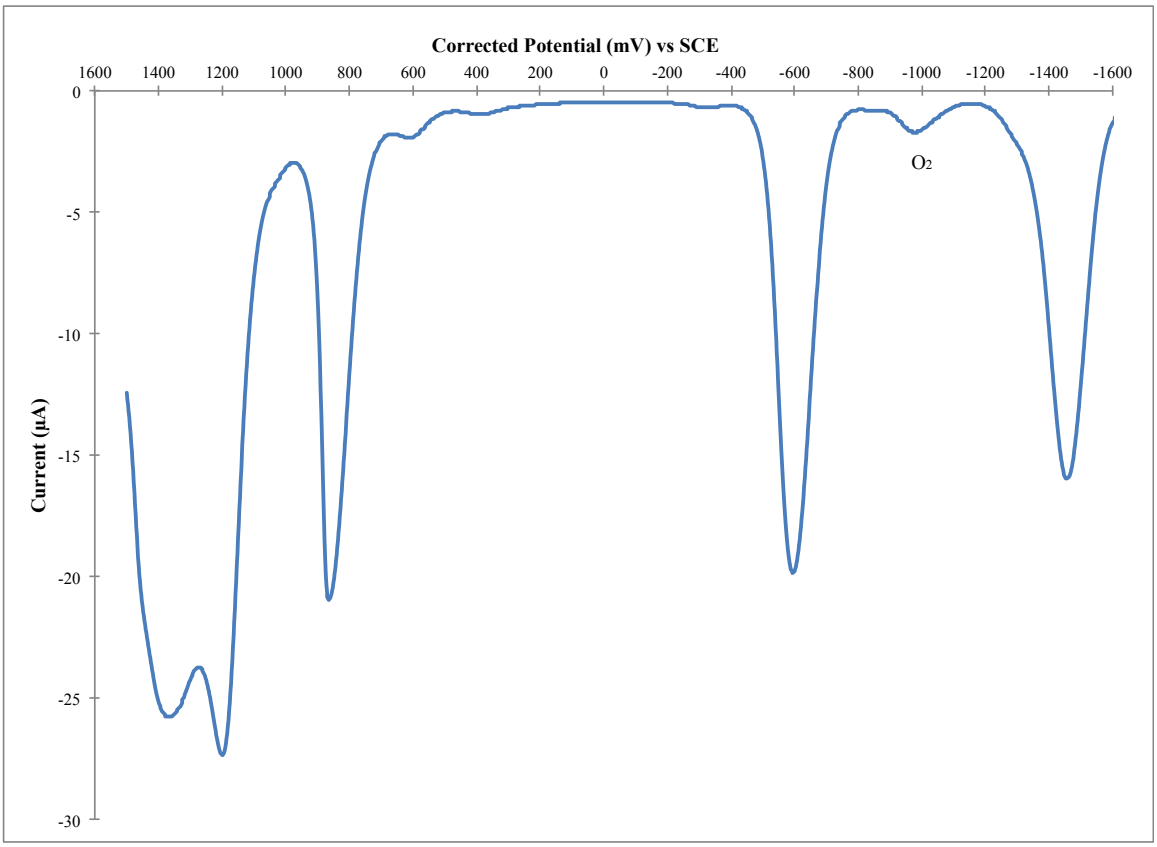

Figure S.39 – Absorption spectra of ligand **1a**, complexes **2a** to **5a** and Aza-BODIPY **6a** in DCM solution.

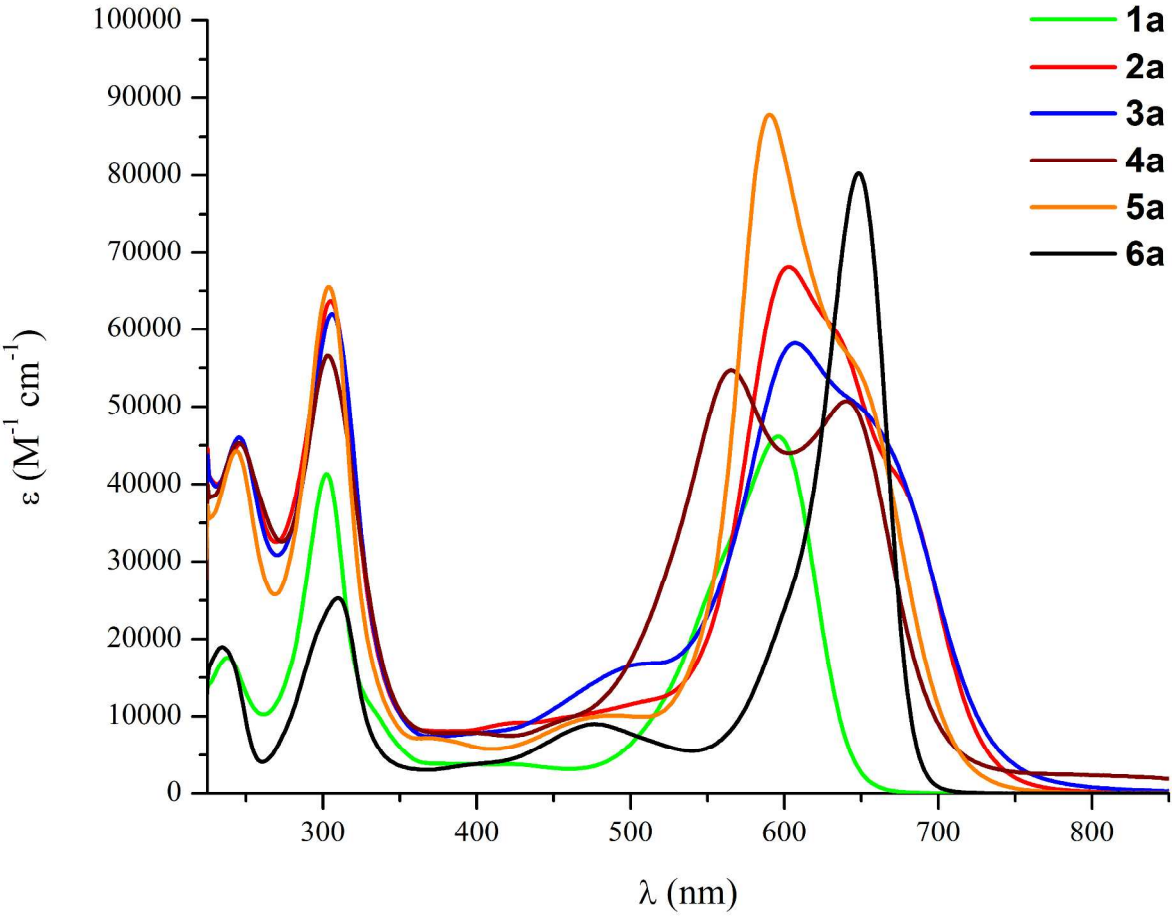

Figure S.40 – Absorption spectra of ligand **1a**, complexes **2a** to **5a** and Aza-BODIPY **6a** in THF solution.

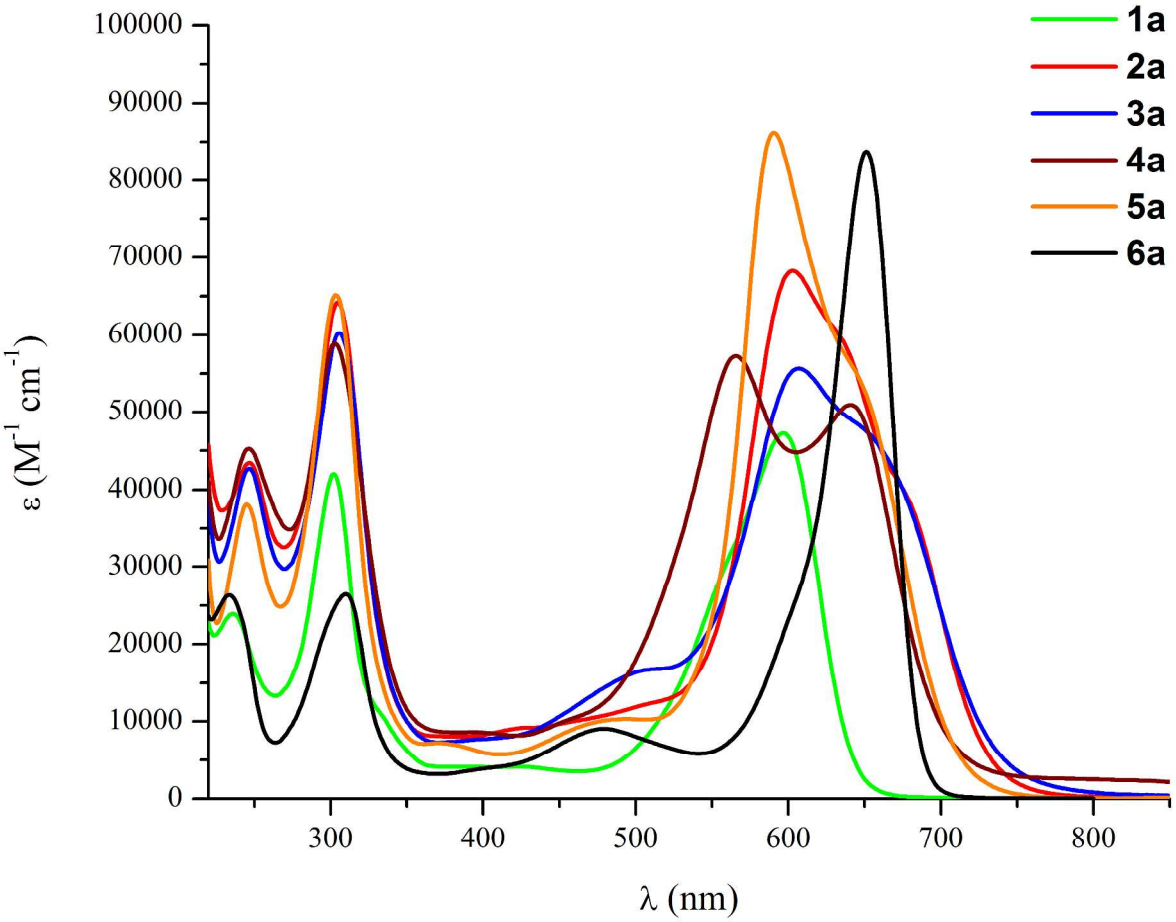

Figure S.41 – Absorption spectra of ligand **1b**, complexes **2b** to **5b** and Aza-BODIPY **6b** in THF solution.

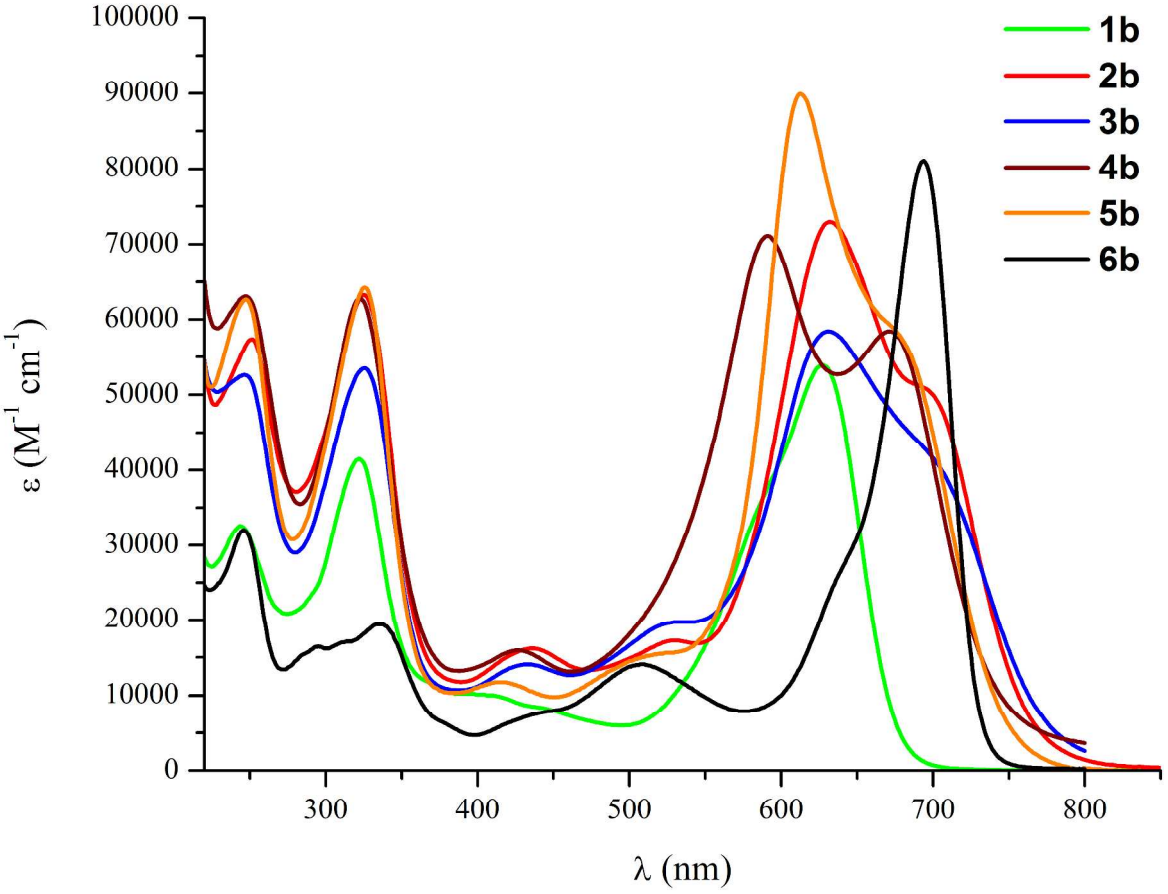

Figure S.42 – Normalized intensity emission spectrum of **1a** and **6a** in DCM solution.

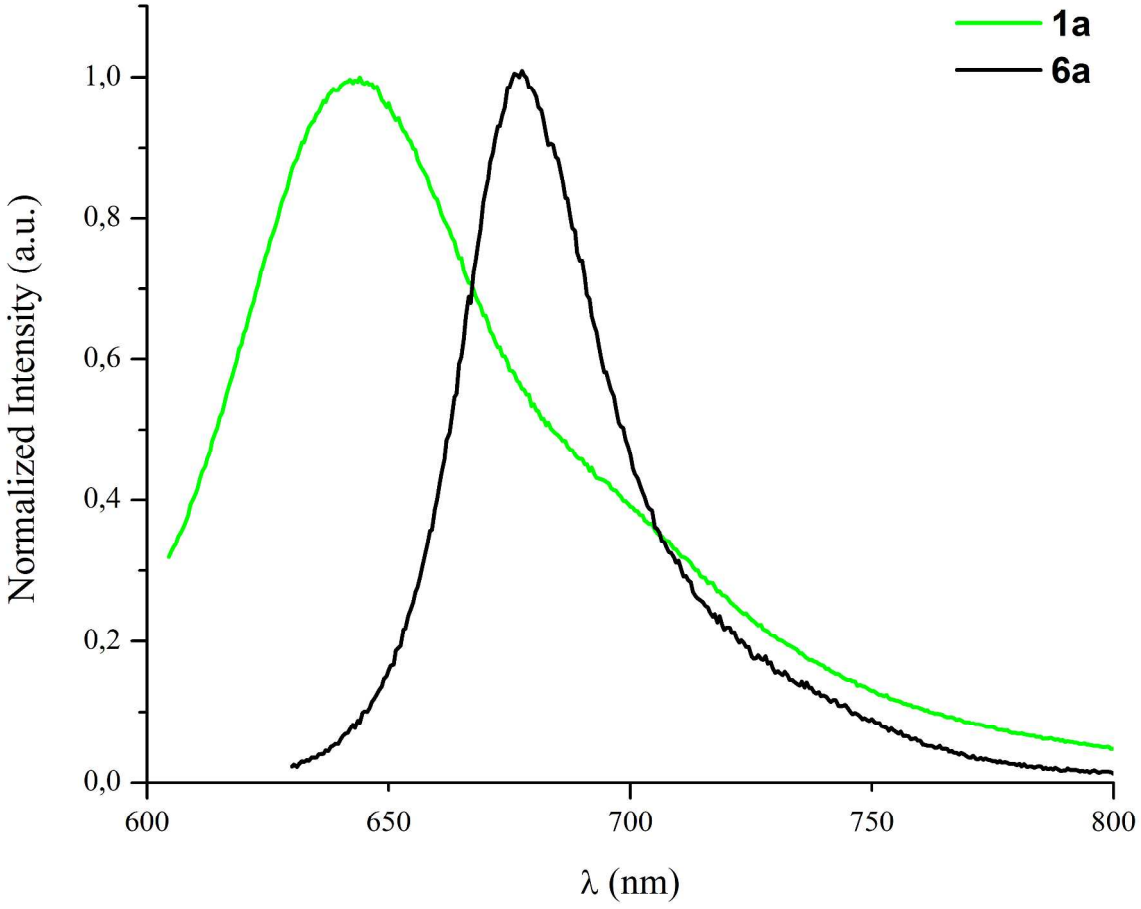

Figure S.43 – Normalized intensity emission spectrum of **1a** and **6a** in THF solution.

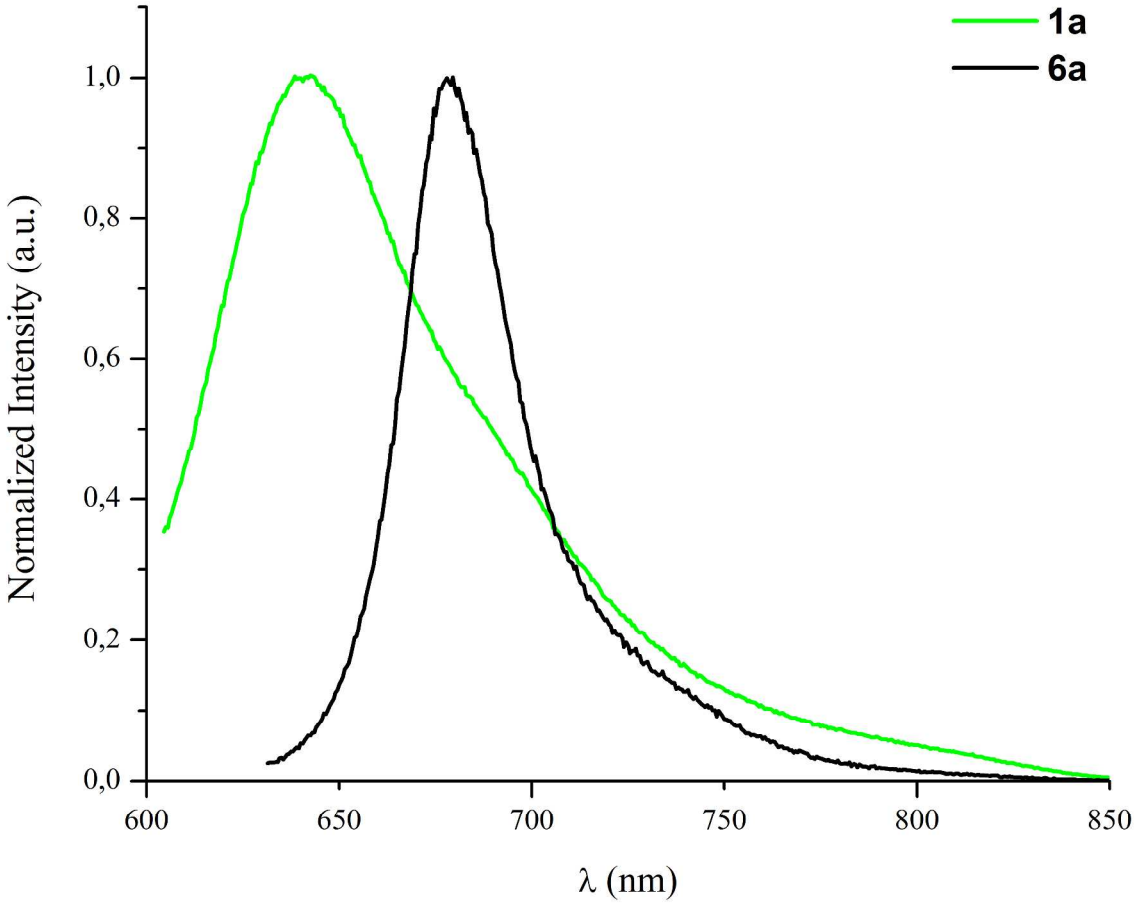

Figure S.44 – Normalized intensity emission spectrum of **1b** and **6b** in THF solution.

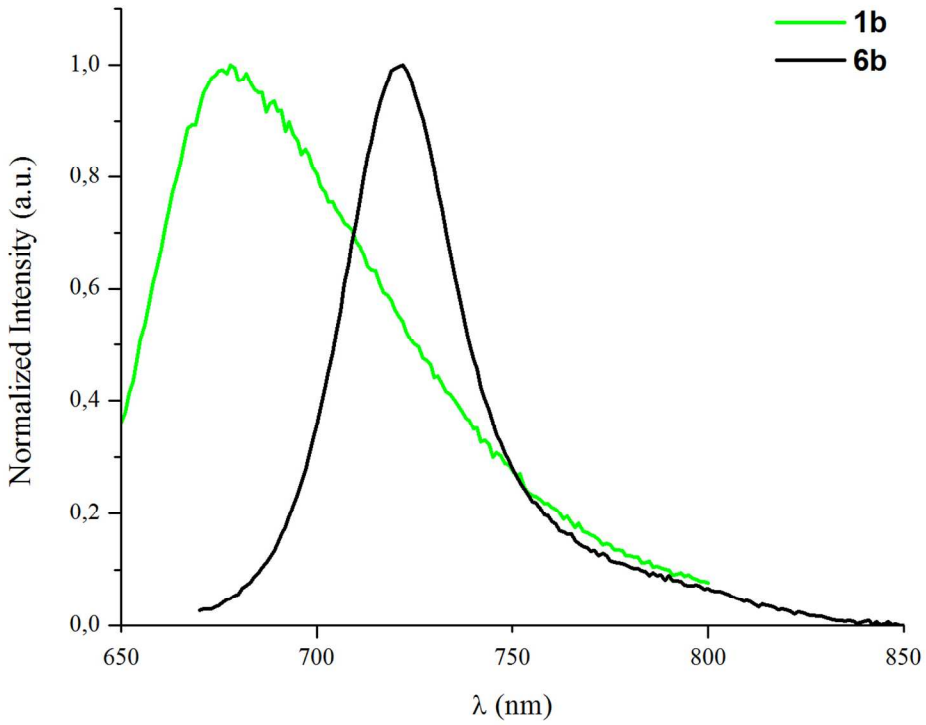

Figure S.45 – Ortep representation of the Co(II) complex **2b** at the 50% probability level.

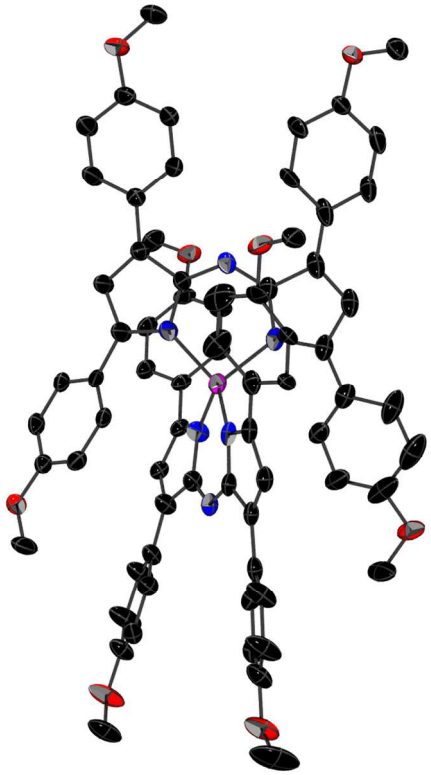

Table S.1 - Crystal Data and Details of the Structure Determination for Ligand **1b** and Co(II) Complex **2b**.

	1b	**2b**
CCDC Number	876955	876954
Formula	$C_{36}H_{31}N_3O_4$	$C_{72}H_{60}N_6O_8Co$
Mw (g/mol); $d_{calcd.}$ (g/cm^3)	569.64; 1.688	1196.19; 1.355
T (K); F(000)	150; 3696	150; 2500
Crystal System	Monoclinic	Monoclinic
Space Group	$P2_1/c$	$P2_1/c$
Unit Cell: *a* (Å)	19.4979(5)	12.2987(3)
b (Å)	7.0104(2)	14.3062(3)
c (Å)	21.2448(5)	34.1066(7)
β (°)	105.288(1)	102.219(1)
V (Å^3); Z	2801.1(1); 4	5865.0(2); 4
θ range (°); completeness	4.32-69.49; 0.991	2.65-69.83; 0.996
Refl.: collec./indep.; R_{int}	37808/5544; 0.052	121155/11031; 0.056
μ (mm^{-1})	0.713	2.822
R1(F); wR(F^2); GoF(F^2) [a]	0.0752; 0.2312; 0.98	0.0610; 0.1686; 1.038
Residual electron density	1.40; -0.37	0.50; -0.63

[a] R1(F) based on observed reflections with I>2σ(I), wR(F^2) and GoF(F^2) based on all data.